

Decision Letter (PHYTO-10-21-0434-R.R1)

From: mtbrewer@uga.edu

To: bcamiletti@gmail.com, plichtenberg@ucdavis.edu, japaredes@ucdavis.edu, thiagoacarraro@gmail.com, jjvelasco@earth.ac.cr, tjmichailides@ucanr.edu

CC: Phytopathology@scisoc.org

Subject: Phytopathology - Decision on Manuscript ID PHYTO-10-21-0434-R.R1

Body: 27-Jan-2022

Dear Dr. Camiletti:

It is a pleasure to accept your manuscript entitled "Characterization of Colletotrichum isolates causing Colletotrichum dieback of citrus in California" in its current form for publication in Phytopathology.

Phytopathology offers a feature called First Look. Within a few days of acceptance, an unedited, unformatted version of your paper can be posted online. At this point, a doi is assigned, and your paper is considered published and is fully citable. This option is not available for Resource Announcements.

When you submitted your new manuscript, you were asked, "Do you want your paper published online prior to print?" If you checked "yes," you should now go to "Manuscripts Accepted for First Look" in your author center. Please upload your First Look version within 48 hours. If you used track changes or inserted comments to the senior editor in the final revision, they should be removed at this point so that a clean version of the manuscript is posted. Please make only cosmetic changes. Do not make changes in the wording of the text, tables, or figure captions or in the figures.

The First Look submission is separate from your final revision submission. Even if you have no changes, you must complete the First Look submission.

The accepted version of the manuscript you submitted through Manuscript Central will be used for editing, not the First Look version and you may make any necessary changes at the galley proof stage. You will not be able to submit any further revisions through Manuscript Central.

Your paper cannot be posted in First Look until these files are received. It will be removed from the First Look site once it has been edited, formatted, and assigned to an issue.


As you may know, we are upgrading our online journals. Your article will now be published in html format with new functionality and features, and improved ease-of-use on computers and mobile devices. Please note, when your galleys are ready for review, a notification from Phytopathology.djs@sheridan.com will be sent, and a notice to review and pay any publication fees from aubilling.djs@sheridan.com. We want you to be aware of these e-mail addresses on behalf of the Phytopathology production team.

We offer significant discounts if the corresponding author of your paper is an APS member. If you are not presently an APS member and would like to join, you can do so by going to our website, <http://www.apsnet.org/about/join/Pages/default.aspx>.

Thank you for your fine contribution. The editors of Phytopathology look forward to your continued contributions to the journal.

Sincerely,
Dr. Marin Brewer
Senior Editor, Phytopathology
mtbrewer@uga.edu

Date Sent: 27-Jan-2022

 Close Window

1 **Characterization of *Colletotrichum* isolates causing *Colletotrichum* dieback of**
2 **citrus in California**

3 Boris X. Camiletti,^{1,†} Paulo S.F. Lichtemberg,¹ Juan A. Paredes,¹ Thiago A. Carraro,¹ Jhordan
4 Velascos,¹ and Themis J. Michailides,^{1,†}

5 ¹ Department of Plant Pathology, University of California Davis, Kearney Agricultural Research
6 and Extension Center, Parlier 93648.

7 †Corresponding author: Boris X. Camiletti, bcamiletti@ucanr.edu; Themis J. Michailides;
8 tjmichailides@ucanr.edu

9
10 **Funding:** Financial support was provided by the Citrus Research Board (Projects #5400-157 and
11 #5400-163).

12
13 **ABSTRACT**

14 Dieback caused by *Colletotrichum* spp. is an emerging disease in California citrus groves. A
15 large-scale survey with emphasis on seasonal variations of latent infections was conducted
16 throughout citrus orchards in Fresno, Kern, and Tulare counties in 2019 and 2020. Latent
17 infections on citrus leaves and twigs varied markedly between years. Isolates of *Colletotrichum*
18 spp. were obtained from asymptomatic tissue and two groups were formed based on colony and
19 spore morphology. The morphological groups were further identified based on multigene sequence
20 analysis using the DNA regions ITS1-5.8S-ITS2, TUB2, and GAPDH. Results revealed that
21 isolates belong to two phylogenetic species, *C. gloeosporioides* and *C. karstii*, being *C. karstii*
22 more frequently isolated. Representative isolates of each species were further selected and
23 characterized based on the response of physiological variables to temperature. Both species had
24 similar optimum growth temperatures but differed in maximum growth rates, with *C.*
25 *gloeosporioides* exhibiting a greater growth rate than that of *C. karstii* on media. Pathogenicity
26 tests on citrus trees demonstrated the ability of *C. gloeosporioides* and *C. karstii* to cause lesions
27 on twigs and no differences in aggressiveness. A fungicide screening performed in this study
28 determined that the DMI fungicides were the most effective in reducing the mycelial growth of *C.*

29 *gloeosporioides* and *C. karstii*. The QoI fungicides showed a remarkably inhibitory impact on
30 spore germination of both species. On average, *C. karstii* was more sensitive to the DMI fungicides
31 than *C. gloeosporioides*. The findings of this study provide new information to understand the
32 *Colletotrichum* dieback of citrus.

33 **Keywords:** mandarin, orange, anthracnose, fungicide sensitivity, pathogenicity, survey,
34 phylogenetic analysis.

35 California leads the fresh citrus market in the United States with a production that accounted
36 for 54% of the nation's citrus crop in the 2019-2020 season and was valued at \$2.3 billion (USDA-
37 NASS 2020). The San Joaquin Valley (SJV) plays a significant role in California's citrus
38 production. In fact, 80% of the mandarin acreage and 94% of Navel orange acreage are distributed
39 in Fresno, Kern, and Tulare counties (Takele 2014). Given the importance of the citrus industry in
40 the SJV, the management of emerging fungal diseases that may threaten the yield and quality of
41 these crops is significant.

42 *Colletotrichum* constitutes an important genus of plant pathogenic fungi that cause destructive
43 diseases, commonly named anthracnose, in several crops worldwide. In citrus production, about
44 25 species of *Colletotrichum* have been documented as pathogens associated with anthracnose
45 diseases of great economic impact. This fungal genus can cause postbloom fruit drop (PFD), key
46 lime anthracnose, post-harvest anthracnose, and other anthracnose diseases that threaten citrus
47 production worldwide (Adaskaveg et al. 2014; Wang et al. 2021; Guarnaccia et al. 2017; Peres et
48 al. 2003; Piccirillo et al. 2018). In California, *C. gloeosporioides* was reported as the causal agent
49 of anthracnose on citrus crops. This pathogen is commonly found colonizing dead tissues, but it
50 may cause disease in high-rainfall years that results in economic losses. Moreover, post-harvest
51 decay is observed when serious epidemics occur before harvest (Adaskaveg et al. 2014).
52 Postbloom fruit drop is an important disease caused by *C. acutatum* and *C. gloeosporioides* species
53 complexes that commonly affect citrus production severely but have not been reported from
54 California (Adaskaveg et al. 2014; Lima et al. 2011; Timmer et al. 1994).

55 The taxonomy of *Colletotrichum* has been historically a challenge due to the numerous
56 obstacles such as the limited distinguishing morphological characters and rare formation of
57 teleomorphic stages (Hyde et al. 2009). A polyphasic approach combining multigene sequencing
58 with morphological, physiological, and pathogenicity characters has been used in impactful studies

59 that changed species concepts in *Colletotrichum* (Cannon et al. 2012; Damm et al. 2012a, 2012b;
60 Weir et al. 2012). These works revealed that *C. acutatum* and *C. gloeosporioides* are species
61 complexes that include numerous species (Damm et al. 2012a; Weir et al. 2012). Most of the
62 species associated with citrus belong to four species complexes: *C. boninense*, *C. acutatum*, *C.*
63 *truncatum*, and *C. gloeosporioides* (Guarnaccia et al. 2017).

64 For the first time, species that belong to the *C. boninense* species complex have been
65 increasingly associated with citrus diseases. The species *C. karstii* is one of the species that belongs
66 to the *C. boninense* species complex. This pathogen has recently received particular attention due
67 to its more frequent association with anthracnose symptoms in citrus, commonly co-infecting
68 tissues with other *Colletotrichum* species (Wang et al. 2021; Guarnaccia et al. 2017; Huang et al.
69 2013). Recent studies reported *C. karstii* as a new pathogen affecting citrus production in the SJV
70 of California. This new pathogen was found to occur in association with *C. gloeosporioides* but
71 causing a disease distinct from the anthracnose attributed to *C. gloeosporioides*. Twig and shoot
72 dieback is the most frequent symptom associated with the disease, although branch dieback and
73 wood canker can be occasionally observed (Mayorquin et al. 2019). This disease, hereafter referred
74 to as *Colletotrichum* dieback, was recently found to be also widespread in Italy and Albania, where
75 symptoms similar to those described in California were observed. Similarly, *C. gloeosporioides*
76 and *C. karstii* were reported as the pathogens responsible for the disease (Riolo et al. 2021).

77 Currently, no management methods exist to mitigate the negative impact of *Colletotrichum*
78 dieback in citrus crops (Mayorquin et al. 2019). However, a variety of management practices are
79 routinely performed to combat diseases caused by *Colletotrichum* spp. on several fruit crops.
80 Although various cultural practices are frequently recommended, chemical control remains the
81 primary option for the farmers to control these pathogens. Commercial products formulated with
82 compounds from different chemical groups, i.e., quinone outside inhibitors (QoI), succinate de-
83 hydrogenase inhibitors (SDHI), sterol demethylation inhibitors (DMI), and chemical multi-site
84 inhibitors (M) are recommended for anthracnose management in California citrus (Adaskaveg and
85 Michailides, 2021). Therefore, these fungicides could also play a significant role in management
86 of *Colletotrichum* dieback. It is well known that the design of fungicides programs against
87 *Colletotrichum* spp. must address differences in fungicide sensitivity. Such variability can be
88 attributed to differences among species as well as among species complexes. Moreover, knowing

89 the fungicide resistance profile of a native *Colletotrichum* population is also crucial to develop
90 management practices that consistently control the disease (Dowling et al. 2020).

91 Little is known regarding the *Colletotrichum* dieback of citrus, and numerous aspects need to
92 be elucidated for the management of this new pathosystem. Pathogen identification, large-scale
93 field sampling, and fungicide sensitivity testing have been proposed as three critical areas that can
94 ultimately lead to the successful management of *Colletotrichum* diseases (Dowling et al. 2020).
95 Thus, the objectives of this study were to (i) conduct a large-scale survey and determine the
96 seasonal variation of *Colletotrichum* spp. incidence in California citrus orchards; (ii) characterize
97 *Colletotrichum* isolates by morphological and molecular characteristics; (iii) assess the
98 pathogenicity of *Colletotrichum* spp. in citrus twigs under field conditions; and (iv) explore the
99 sensitivity of *Colletotrichum* spp. to commercial fungicides.

100 MATERIALS AND METHODS

101 **Field survey and pathogen isolation.** A two-year survey was conducted in commercial citrus
102 orchards throughout Fresno Co. (10 orchards), Kern Co. (20 orchards), and Tulare Co. (19
103 orchards) in the 2018/2019 and 2019/2020 seasons. The survey periods started in November and
104 ended in August next year and are hereafter referred to as 2019 and 2020. Of the 49 sampled
105 orchards, 17 were planted with orange cultivars (Atwood, Cara Cara, Fukumoto, and Washington),
106 26 with mandarin cultivars (Gold Nugget, Clemenules, Tango, W. Murcott, Owari Satsuma, and
107 Sumo), and 6 with lemon cultivars (Lisbon and Meyer). Each site was sampled during winter (from
108 November to January), and 19 of them randomly selected were re-visited during spring
109 (April/May) and summer (July/August) to monitor pathogen incidence. Climatic data pertinent to
110 the survey were obtained from the California Irrigation Management Information System (CIMIS
111 2021). During each sampling, asymptomatic twigs ($n=30$) and leaves ($n=60$) were randomly
112 collected and stored at 4°C until analysis. To obtain fungal isolates infecting asymptomatic twigs,
113 the plant material was cut into 10-mm sections until approximately 10 parts per twig were obtained.
114 Plant tissue was surface-disinfested by submerging in 0.5-0.6% sodium hypochlorite (10% Clorox
115 bleach; The Clorox Company, Oakland, CA) for 4 min and air-dried on an aseptic surface in a
116 laminar flow hood for 30 min. Parts of twigs were then placed onto acidified PDA (LA, 2.5 ml
117 lactic acid 25% v/v) and incubated at 25 °C for 7 days. Plates were examined after the growing
118 period and fungal colonies presenting morphological characteristics (growth pattern, color, and

119 conidia shape) consistent with *Colletotrichum* were counted. The number of parts with latent
120 infections was recorded and results were expressed as incidence (percentage of infected sections).
121 The asymptomatic leaves were disinfested as previously indicated for twigs and examined using
122 the overnight freeze incubation technique (ONFIT) according to Pryor and Michailides (2002).
123 Briefly, plant material was placed into humid plastic chambers (30 cm × 21 cm × 10), held at -15-
124 16°C for 24 h, and incubated at room temperature for 7 to 10 days. *Colletotrichum* colonies that
125 erupted from the leaf tissue were identified by observing colony characteristics and spore
126 morphology, as previously described, and the number of latent infections per leaf was determined.
127 Pure cultures obtained from colonies randomly selected throughout the experiment were used to
128 obtain single-spore cultures. Serial dilutions were prepared by collecting masses of spores from
129 colonies with developed acervuli and spreading them onto water-agar (1.5% agar) plates. After
130 incubation at 25°C for 12-16 h, isolated germinating conidia were visualized using a
131 stereomicroscope and transferred to new PDA plates.

132 **Morphological and physiological characterization.** A total of 102 single-spore cultures
133 obtained during the survey were initially divided into two morphological groups considering
134 colony color and spore shape (Table S1). Morphological characteristics of both groups were
135 contrasted with published descriptions of *Colletotrichum* species associated with twigs and shoot
136 dieback in California citrus orchards (Mayorquin et al. 2019). Fifteen isolates per group were
137 further characterized by the growth rate, sporulation, and spore morphology (Table S1). Mycelial
138 plugs (5 mm) were collected from the periphery of 5-day-old colonies and placed in the center of
139 Petri plates (90 mm) containing PDA. Plates were incubated at 25°C in darkness and the diameter
140 of each colony was measured using a digital caliper after 3, 5, and 7 days of incubation. Mean
141 values were transformed to the daily growth rate (mm per day) and the 7-day average was
142 calculated for each isolate. After measuring colony diameter, 5 ml of sterile deionized water was
143 added to each plate, and spores were suspended by scraping the colony from the PDA surface with
144 a sterile inoculating loop. The suspensions were aseptically filtered through a double-layered
145 cheesecloth to remove mycelium and transferred to glass vials (20 mL). The spore concentrations
146 were determined using a Neubauer chamber and adjusted according to their respective colony sizes
147 (spores per cm²). Finally, 5- μ l drops of the spore suspensions were mounted in microscope slides
148 and the size of 100 conidia was examined using a Leica compound microscope (Leica DM2000
149 LED Microscope, Wetzlar, Germany). The length and width of each conidium were measured, and

150 their volume was calculated according to Moral et al. (2021). The entire experiment was conducted
151 twice with three replicates per isolate.

152 **DNA extraction and amplification.** Nineteen single-spore cultures from both morphological
153 groups were randomly selected and used for molecular characterization. Mycelium and conidia
154 from cultures grown on Potato Dextrose Broth (BD, Franklin Lakes, NJ) at 25°C in darkness for
155 7 days were used for DNA extraction. Total DNA was extracted using the FastDNA kit and
156 FastPrep Instrument (MP Biomedicals, Santa Ana, CA) following the manufacturer's instructions.
157 The concentration and purity of the DNA template were determined with a NanoDrop 2000c
158 spectrophotometer (Thermo Fisher Scientific, Wilmington, DE) and adjusted to a concentration of
159 5 ng ml⁻¹. Three genomic regions were amplified and sequenced as recently performed by
160 Mayorquin et al. (2019): the ITS1-5.8S-ITS2 regions of the rDNA locus using primers ITS4 and
161 ITS5 (White et al. 1990); a portion of the nuclear beta-tubulin gene (TUB2) using primers T1 and
162 Bt2b (White et al. 1990); and part of the glyceraldehyde-3-phosphate dehydrogenase gene
163 (GAPDH) with primers GDF1 and GDR1 (Guerber et al. 2003). Polymerase chain reactions (PCR)
164 amplification were carried out in an Arktik Thermocycler (Thermo Fisher Scientific, Wilmington).
165 Reaction mixtures contained 12.5 µL of AccuPower PCR Premix (Bioneer, Alameda, CA), 0.25
166 µL of each primer at 10 µmol l⁻¹, and templated DNA ranging from 2 to 4 µL. DNase-free water
167 was added to reach a final volume of 25 µL per reaction. For TUB2, 0.15 µL of each primer was
168 added. For ITS, cycling conditions were as described by Mayorquin et al. (2019). For GAPDH,
169 cycling conditions were as follow: an initial preheat at 95°C for 2 min, followed by 35 cycles of
170 denaturation at 94°C for 1 min, annealing at 60°C for 1 min, and extension at 72°C for 3 min,
171 followed by a final extension at 72°C for 7 min. For TUB2, the annealing temperature was adjusted
172 to 55°C. PCR products were purified with ExoSAP-IT (Affymatrix Inc., Santa Clara, CA)
173 following the manufacturer's protocol. Purified products were sequenced in both directions at the
174 UC-Davis sequencing facility.

175 **Multilocus phylogenetic analysis.** The nucleotide sequences were blasted against the
176 GenBank nr database, with searches restricted to type materials for initial identification of the
177 closest matching species and species complexes. *C. gloeosporioides* and *C. boninense* species
178 complexes were identified and sequences from recent publications available at GenBank were
179 obtained (Weir et al. 2012; Damm et al. 2012b; Marin-Felix et al. 2017; Mayorquin et al. 2019).

180 Other authors (Weir et al. 2012; Damm et al. 2012b) demonstrated that genomic areas selected in
181 this study were combinable. Thus, the phylogenetic analysis was carried out using a combined
182 dataset with multilocus sequences obtained from concatenated genes. Sequences from isolates
183 belonging to the same species complex were aligned in MAFFT v7 online server
184 (<https://maf.cbrc.jp/alignment/server/>) (Kato and Standley, 2013), and manually adjusted, when
185 necessary, with the MEGA7 software (Kumar et al., 2016). Phylogenetic analyses were performed
186 in the PhyloSuite v1.2.2 (Zhang et al., 2019) using two different approaches: Maximum Likelihood
187 (ML) analysis with IQ-TREE and Bayesian Inference (BI) analysis with MrBayes v3.2.6 (Ronquist
188 and Huelsenbeck, 2003). Evolutionary models were tested using ModelFinder (Kalyaanamoorthy
189 et al., 2017) and the best-fit substitution model for each gene was selected based on the Akaike
190 Information Criterion corrected. For ML analysis, evolution was simulated until likelihood scores
191 converged. An ultrafast bootstrap approach (UFBoot) was performed with 1000 pseudoreplicates
192 to estimate the statistical support of the branches. Nodes with zero branch lengths were collapsed.
193 For BI, analysis was performed using two parallel runs and sampling every 10,000 generations;
194 each of the two parallel runs had one cold and three heated chains and were run until split
195 frequencies were less or equal to 0.01. The first 25% of the generated trees were discarded as burn-
196 in before calculating the 50% majority consensus trees for ML and posterior probability values for
197 BI. The resulting trees from both analyses were visualized in the program FigTree v. 1.4.3
198 (www.tree.bio.ed.ac.uk/software/figtree/) and their topologies were compared. We assessed
199 possible incongruences and conflicts between clades with significant posterior
200 probability/bootstrap support in both analyses and compared their topologies with those presented
201 in previously published phylogenies of *Colletotrichum* (Damm et al., 2012b; Weir et al., 2012). In
202 the phylogenetic tree, the clades were considered when posterior probability values were above
203 0.9 for BI analysis and when bootstrap values were above 80% for ML analysis. Sequences
204 obtained in this study were deposited in GeneBank (Table 1).

205 **Effect of temperature on mycelial growth.** Studies were carried out using six molecularly
206 identified isolates of *C. karstii* (13J74, 13J89, and 13F29) and *C. gloeosporioides* (13I58, 13I46,
207 and 13J85), hereafter referred to as representative isolates. Petri plates were prepared as detailed
208 in section 2.2 and incubated at 10, 15, 20, 25, 30, and 35°C in darkness. The diameter of each
209 colony was measured using a digital caliper after 3, 5, and 7 days of incubation, and data were
210 transformed to growth rate. Three plates per combination of isolate and temperature were prepared,

211 and the assay was conducted three times. At the end of each experiment, mycelial plugs that did
212 not result in fungal growth at 35°C were replated on PDA and incubated at 25°C for 10 days to
213 corroborate possible resilience growth. The optimum growth temperature and maximum growth
214 rate were calculated for each isolate using the Analytis Beta Model according to Moral et al.
215 (2012).

216 **Effect of temperature on spore germination and appressorium formation.** Spore
217 suspensions of the representative isolates were prepared by collecting masses of spores from 7-
218 day-old cultures actively growing on LA. The spore density was determined as indicated above
219 and adjusted to a final concentration of 10^5 conidia ml⁻¹. Aliquots (100 µl) of spore suspensions
220 were aseptically spread on WA, and the plates were incubated in the dark at 10, 15, 20, 25, 30, and
221 35°C. After 12 h of incubation, the percentage of germinated spores was calculated by observing
222 100 conidia randomly selected using a microscope. Spores were scored as germinated when the
223 germ tube had a size of at least the length of the conidia. Immediately after recording spore
224 germination, plates were incubated at the condition described above for another 12 h to allow
225 appressorium formation. At the end of the incubation period, plates were again examined and the
226 percentage of germinated spores ($n=50$) that produced appressoria was recorded. A set of 3 plates
227 was prepared for each treatment and the experiment was repeated two times.

228 **Pathogenicity test.** The experiment was performed in a navel orange (cv. Washington) orchard
229 located at the Bayer Crop Science experimental facilities near Fresno, CA. Five trees were
230 inoculated with 30 isolates belonging to the species complex *C. gloeosporioides* and *C. karstii*
231 (Table S1). Spore suspensions containing 1×10^5 spores ml⁻¹ were prepared from 2-week-old
232 cultures, as previously described. In each tree, one twig per isolate was wounded with a cork borer
233 (5 mm) and inoculated with 15 µl of the respective spore suspension; sterile water was used to
234 inoculate the shoots of the control treatment. Wounds were finally wrapped with parafilm. Twigs
235 were sampled 15 months after inoculations (April 2019 to June 2020) and the internal vascular
236 necrosis (lesions) was measured. To reisolate the pathogen, small sections were removed
237 aseptically from the margins of the resulting lesions and plated onto PDA as described above.

238 **Fungicide sensitivity evaluation.** *Fungicides.* Commercial fungicide products listed in Table
239 2 were chosen based on their potential use for the management of *Colletotrichum* dieback in
240 California citrus.

241 *Mycelium growth.* The fungicides fluopyram, penthiopyrad, metconazole, tebuconazole,
242 chlorothalonil, and Cu hydroxide were assessed by their effects on mycelial growth of *C.*
243 *gloeosporioides* and *C. karstii*. Initially, all the fungicides were evaluated against 53 isolates (*C.*
244 *gloeosporioides*, $n=21$; *C. karstii*, $n=32$) using the agar dilution method. In this experiment, the
245 final fungicide concentrations evaluated were 0 (control), 1, and 10 $\mu\text{g ml}^{-1}$. Stock suspensions
246 were prepared in sterile distilled water and added to PDA, previously cooled to 45-50°C after
247 sterilization. Petri plates (90 mm) containing media supplemented with the fungicide at each of
248 the concentrations were inoculated with mycelial plugs as indicated above. Mycelial growth was
249 measured after 7 days of incubation at 25°C, as described above. Relative growth inhibition (RGrI)
250 was calculated according to the following formula: $\text{RGrI} = [(D_{\text{control}} - D_{\text{Treatment}}) / D_{\text{control}}] \times 100$, where
251 D =diameter of the colony. Three plates per combination of isolate-fungicide-concentration were
252 prepared and the experiment was repeated once.

253 The effect of the fungicides on mycelial growth was also evaluated using the spiral gradient
254 dilution method according to Förster et al. (2004), with minimum modifications. Briefly, spore
255 suspensions of 16 randomly selected isolates per fungal species were prepared as indicated above.
256 Autoclaved wood stirrers (5cm) were placed onto LA plates, seeded with aliquots of spore
257 suspension (100 μl each), and incubated at 25 °C for 5 days. Petri dishes (150 mm in diameter)
258 were prepared with 50 ml of PDA, except for SDHI fungicides where YBA was used. Aqueous
259 stock suspensions were prepared for each fungicide at the appropriate concentration. Each
260 fungicide suspension was spirally applied to the surface of its respective medium with a spiral
261 plater (Eddy Jet 2W, IUL, Barcelona, Spain) using the exponential mode of application (Exp. 3000
262 M 54.30 μl). Plates containing non-amended media were used as control. One mycelium-covered
263 wood stirrer per isolate was placed on the agar surface, with the mycelium facing down, and across
264 the fungicide gradient. Two replicate plates were prepared for each fungicide with a maximum of
265 eight stirrers per plate. Plates were incubated at 25°C for 3 days. After incubation, the point where
266 mycelial growth was inhibited by 50% with respect to fungal growth on the control plates, was
267 marked. The distance between this point and the center of the plate was used to determine the 50%
268 effective fungicide concentration (EC_{50}) using the ECX package (Torres-Londoño et al. 2016) and
269 the statistical software R version 4.0.3 (RStudio Team 2020).

270 *Spore germination.* The QoI and SDHI fungicides listed in Table 2 were assessed separately by
271 their effects on spore germination. The experiments were carried out using spore suspensions of
272 the 53 isolates indicated above. Stock suspensions were prepared in sterile distilled water and
273 added to previously cooled (45-50°C) YBA to obtain final concentrations of 0 (control), 1, and 10
274 $\mu\text{g ml}^{-1}$. To block the alternative respiration pathway, salicylhydroxamic acid (SHAM) was added
275 to QoI-supplemented YBA at 100 $\mu\text{g ml}^{-1}$. Spore suspensions (1×10^5 conidia ml^{-1}) were prepared
276 from 7-day-old cultures. Aliquots (100 μl) of spore suspensions were aseptically spread on the
277 YBA plates. After 12 h of incubation at 25°C, the percentage of germinated spores was determined
278 as previously indicated. Three plates per combination of isolate-fungicide-concentration were
279 prepared and the experiment was repeated once.

280 **Statistical analysis.** For each experiment, data from repetitions were combined after checking
281 for homogeneity of the experimental error variance for each variable with the *F* test. Proportions
282 of species within the *Colletotrichum* population were compared using the Chi-square test. Data
283 sets for optimum growth temperature and maximum growth rate were subjected to analysis of
284 variance (ANOVA), and means were compared using Fisher's protected least significant difference
285 test (LSD) at $P < 0.05$. The mean EC_{50} values for *C. gloeosporioides* and *C. karstii* were compared
286 for each fungicide using two-tailed *t* tests with $\alpha = 0.05$. The remaining data did not satisfy
287 assumptions of homogeneity of variances and normality when examined. Consequently, the
288 Kruskal-Wallis one-way nonparametric test was performed on these data, and means were
289 compared at $P = 0.05$. Spearman rank correlation was used to study monotonic relationships
290 between temperature and conidial germination, and between temperature and appressoria
291 formation. Statistical analysis was performed using the InfoStat software v. 2020 and the statistical
292 software RStudio v. 4.1.0.

293

RESULTS

294 **Incidence of latent infections.** Twigs and leaves were examined for latent infections of
295 *Colletotrichum* spp. during winter, spring, and summer in 2019, and during winter and summer in
296 2020 (Fig. 1). No significant differences ($P = 0.166$) were found among the three counties and data
297 were combined. Consequently, a prevalent county with higher infections was difficult to
298 determine. Rainfall episodes occurred more frequently during the first survey year than during the
299 subsequent year (23 vs 14 episodes, respectively). In Fresno Co., the rainfall intensity during the

300 winter and spring months was 251 mm in 2019 and 190 mm in 2020. The same pattern was
301 reported for Tulare Co. (259 mm in 2019 vs 223 mm in 2020). Incidence of latent infections on
302 twigs varied significantly between years, presenting higher values during 2019 than during 2020
303 (9.62 ± 0.73 vs 1.91 ± 0.95). During 2019, latent infections were significantly higher in twigs from
304 orange orchards than twigs from mandarin orchards in each season, whereas no significant
305 differences ($P=0.233$) were found during the subsequent year. No significant seasonal variation
306 was observed for latent infection on twigs during 2019 ($P=0.805$) and 2020 ($P=0.946$). Latent
307 infections in citrus leaves matched the pattern observed for twigs and significantly higher values
308 were observed in 2019 than in 2020 (3.18 ± 0.58 vs 0.55 ± 0.67). However, no significant differences
309 were observed between orange and mandarin orchards, except during the summer season in 2019
310 when a higher incidence was observed for orchards planted with orange cultivars. Although
311 seasonal variations were observed, no significant differences were detected within both survey
312 periods.

313 **Morphological and physiological characterization.** The isolates of *Colletotrichum* obtained
314 during the survey matched the morphological characteristics described by Mayorquin et al. (2019)
315 for *C. gloeosporioides* and *C. karstii* affecting citrus twigs and shoots and were classified
316 accordingly as *C. gloeosporioides* and *C. karstii*. Based on this classification, *C. karstii* was more
317 frequently isolated than *C. gloeosporioides* (79% vs 21%; $Df= 1$; Chi-Square = 32.9; $P<.05$). The
318 daily growth rate on PDA exhibited significant differences between the morphological groups.
319 Isolates of *C. gloeosporioides* presented growth rates ranging from 4.5 to 9.7 mm per day, with a
320 mean growth rate of 7.2 ± 1.0 mm per day. Isolates of *C. karstii* showed growth rates ranging from
321 2.5 to 8.2 mm per day, with a mean growth rate of 5.9 ± 1.1 mm per day. In addition, *C.*
322 *gloeosporioides* showed a significantly higher sporulation rate than *C. karstii* (Table 3). Conidial
323 dimensions also showed significant differences between the morphological groups (Table 3).

324 **Multilocus phylogenetic analysis.** Eight isolates, previously classified as *C. karstii* based on
325 morphological characteristics, belonged to the *C. boninense* species complex. To analyze this
326 complex, the eight isolates together with 30 reference isolates, including the outgroup *C.*
327 *gloeosporioides* (ICMP 17821), were used to construct phylogenetic trees with the ITS region and
328 partial genes sequences of GAPDH and TUB2. The final data matrix contained a total of 935
329 characters with gaps (ITS: 1-453, GAPDH: 454-665, TUB2: 666-935). For BI and ML analyses,

330 the selected models were SYM + I + G4 for ITS and TUB2, and K2P + I for GAPDH. The
331 consensus tree obtained from ML analysis confirmed the tree topology obtained with BI. Ultrafast
332 bootstrap support values agreed with Bayesian posterior probability. The eight isolates were
333 grouped with specimens of *C. karstii* isolated from California citrus and reference isolates in a
334 distinct clade with significant statistical support in the multilocus phylogenetic analysis (1/97,
335 BI/ML), as shown in Fig. 2. Eleven isolates morphologically classified as *C. gloeosporioides* were
336 also classified as this species complex. To analyze this complex, the eleven isolates together with
337 61 reference isolates, including the outgroup *C. boninense* (CBS 123755), were used to construct
338 phylogenetic trees as previously detailed. The final data matrix contained a total of 975 characters
339 with gaps (ITS: 1-475, GAPDH: 476-674, TUB2: 675-975). For BI and ML analyses, the selected
340 models were SYM + I + G4 for ITS and TUB2, and K2P for GAPDH. The consensus tree obtained
341 from ML analysis confirmed the tree topology obtained with BI. Ultrafast bootstrap support values
342 agreed with Bayesian posterior probability. The eleven isolates of the present study were grouped
343 with reference isolates of *C. gloeosporioides*, including specimens from California citrus, in a
344 distinct clade with significant statistical support in the multilocus phylogenetic analysis (1/100,
345 BI/ML), as shown in Fig. 3.

346 **Effect of temperature on mycelial growth.** The temperature influenced the mycelial growth
347 rate of the representative isolates. All isolates grew on PDA when incubated at temperatures
348 ranging from 15 to 30°C, but some isolates failed to grow at 10 or 35°C. However, the maximum
349 temperature evaluated was not lethal for the representative isolates since mycelial plugs resulted
350 in mycelial growth when they were replated and incubated at 25°C. Isolates of *C. karstii* showed
351 a similar growth pattern, and a similar behavior was observed for the isolates of *C. gloeosporioides*
352 (Table 4). The optimum growth temperature estimated by the model was 23.4°C for both species,
353 evidencing no significant differences between them (Fig. 4). Regarding the maximum growth rate,
354 the statistical analysis indicated that one of the representative isolates of *C. gloeosporioides* differs
355 from the others (Table 4). Moreover, significant differences were found when the data for each
356 species were combined, and the mean values were compared. According to the model, *C.*
357 *gloeosporioides* showed a maximum growth rate significantly higher than *C. karstii* (10.5 ± 1.5 vs
358 8.1 ± 0.3 mm day⁻¹, respectively).

359 **Effect of temperature on conidial germination and appressorium formation.** The effects
360 of temperature on conidial germination and appressorium formation of *C. gloeosporioides* and *C.*
361 *karstii* are shown in Fig. 5. Conidial germination of *C. gloeosporioides* isolates occurred after 12
362 h at all temperatures studied. The magnitude of this process was significantly affected by the
363 temperature. All isolates of *C. gloeosporioides* showed a similar pattern, in which the percentage
364 of germinated conidia increased ($r_s = 0.80, P < .05$) simultaneously with the temperature, and the
365 significantly highest values were observed at 35°C. At this temperature, the isolates 13J85 and
366 13I46 showed percentages of germinated conidia (54 and 51%, respectively) significantly higher
367 than the isolate 13J85. Conversely, the percentage of germinated conidia that produced appressoria
368 was negatively correlated ($r_s = -0.56, P < .05$) with temperature, and the significantly highest rates
369 were observed at temperatures between 10 and 20°C, with no significant differences among them.
370 In fact, any of the germinated conidia resulted in appressorium formation when were incubated at
371 35°C. Isolates of *C. karstii* germinated and formed appressoria after 12 h at all temperatures
372 evaluated. Both processes varied significantly with the temperature, with nonmonotonic
373 dependence. Maximum germination and appressorium formation occurred at 20 and 25°C, with
374 no significant differences among them. At these temperatures, isolate 13J74 had a conidial
375 germination rate significantly lower than the rest of the isolates, which did not differ between them.
376 On average, *C. karstii* had germination and appressorium formation rates (48 ± 22 and 64 ± 27 %, respectively) significantly higher than *C. gloeosporioides* (24 ± 15 and 39 ± 31 %, respectively).

378 **Pathogenicity tests.** Under field conditions, all the isolates of *C. gloeosporioides* and *C. karstii*
379 caused internal vascular necrosis on the twigs 15 months after inoculation. The lesions produced
380 by both species were brown and extended from both sides of the wounds. In this trial, *C.*
381 *gloeosporioides* produced lesions that averaged 13.80 ± 5.4 mm in length, while *C. karstii* caused
382 lesions with a mean length of 14.01 ± 8.6 mm. No significant differences ($P = 0.7704$) in lesion
383 lengths were observed between the *Colletotrichum* species and none of the isolates caused twig or
384 shoot dieback after the evaluated period. No significant intraspecific variability was observed
385 among isolates of *C. gloeosporioides* and *C. karstii*. No lesions were observed in the control
386 treatment and all isolates were reisolated from symptomatic twigs.

387 **Fungicide sensitivity evaluation. Mycelium growth.** The effect of six fungicides on the
388 mycelial growth of *C. gloeosporioides* and *C. karstii* populations isolated from citrus is shown in

389 Fig. 6. The systemic fungicides metconazole and tebuconazole were highly effective in inhibiting
390 the mycelial growth of both pathogen populations, and all *Colletotrichum* isolates were sensitive
391 to both active ingredients. Of the 32 *C. karstii* isolates, only one isolate was inhibited <50% by the
392 lowest rate of metconazole and tebuconazole when compared to the control treatment. Among the
393 21 isolates of *C. gloeosporioides*, 3 showed percentages of inhibition of mycelial growth below
394 50% when both fungicides were evaluated at the lowest concentration. Overall, the fungicide
395 penthiopyrad presented an intermediate antifungal activity. A wide range of growth inhibition was
396 observed in plates amended with this fungicide. For example, the highest concentration of
397 penthiopyrad caused inhibitions that ranged from 11 to 89% for *C. karstii* and from 0 to 94% for
398 *C. gloeosporioides*. In addition, approximately 50% of the *Colletotrichum* isolates were inhibited
399 >50% by this fungicide when evaluated at this rate. The remaining fungicides were the least
400 effective in inhibiting the mycelial growth of both pathogen populations. Among the
401 *Colletotrichum* isolates included in this assay, only five isolates were inhibited >50% by
402 chlorothalonil at the highest concentration evaluated, while Cu hydroxide showed scarcely any
403 efficacy against the isolates. It should be noted that the fungicide penthiopyrad was more effective
404 at both concentrations tested than the other SDHI fungicide, fluopyram. Similar results were
405 obtained when the sensitivity of *C. gloeosporioides* and *C. karstii* to the fungicides were
406 determined using the spiral gradient dilution method (Fig. 7). The DMI fungicides, metconazole
407 and tebuconazole, had high activity against the mycelial growth of all the *Colletotrichum* isolates,
408 with EC₅₀ values that ranged from 0.03 to 0.90 µg ml⁻¹. A wide range of sensitivity was observed
409 for the fungicide penthiopyrad, from 0.30 to 7.42 µg ml⁻¹. Based on the EC₅₀ values, *C. karstii*
410 showed a significantly higher sensitivity to tebuconazole, metconazole, and chlorothalonil, while
411 *C. gloeosporioides* was more sensitive to penthiopyrad. No significant differences were found
412 between the species for the fungicides Cu hydroxide and fluopyram.

413 *Spore germination.* The percentage of germinated conidia in the control plates showed a wide
414 range, from 34 to 98% among isolates of *C. gloeosporioides* and from 22 to 96% among isolates
415 of *C. karstii*. The addition of SHAM at 100 µg/ml did not significantly affect the spore germination
416 of the *Colletotrichum* isolates. Spore germination of all *Colletotrichum* isolates was completely
417 inhibited by azoxystrobin at both concentrations, except for one isolate of *C. karstii* that showed a
418 germination rate of 16% with respect to the control when exposed at the lowest concentration
419 tested. The same pattern was observed for trifloxystrobin, where the same isolate had a relative

420 germination rate of 9%. Conversely, the SDHI fungicides had scarcely any efficacy against the
421 conidial germination of the *Colletotrichum* isolates evaluated in this assay. Only two isolates of *C.*
422 *karstii* and two isolates of *C. gloeosporioides* were sensitive to penthiopyrad, in which spore
423 germination was inhibited by 33-55% and 24-32%, respectively, when compared to the control
424 treatment. Only one *C. karstii* isolate was sensitive to fluopyram, in which spore germination was
425 inhibited by 42 and 56% with respect to the control treatment, when exposed at 1 and 10 µg/ml,
426 respectively.

427

DISCUSSION

428 The *Colletotrichum* dieback was first characterized as a new disease of citrus in California and
429 further reported in the Mediterranean region. In both studies, the disease was attributed to *C.*
430 *gloeosporioides* and the newly reported species *C. karstii* (Mayorquin et al. 2019; Riolo et al.
431 2021).

432 In this study, a large-scale survey with emphasis on seasonal variations of latent infections was
433 conducted throughout orchards in Fresno, Kern, and Tulare counties. Latent infections on citrus
434 leaves and twigs varied markedly between years. Higher incidence values were found during the
435 first year of the survey when citrus orchards had more conducive conditions than the subsequent
436 year. It is well-known that the epidemiology of *Colletotrichum* infections is influenced by
437 environmental conditions, especially precipitation and relative humidity. Conidia are spread by
438 rain and infection of plant tissues is favored by moist conditions (Yang et al. 1990; Smith 2008).
439 In the SJV, precipitations events are typically concentrated in the winter and spring months (Lovatt
440 2014). Previous studies indicated that spore trapping of *Colletotrichum* species in citrus orchards
441 was more frequent during these months (Mayorquin et al. 2019). However, this phenomenon
442 seems not to influence the incidence of latent infections since no seasonal patterns were observed
443 in our study. Latent infections were found throughout the season showing that healthy tissues are
444 a potential source of inoculum when favorable environmental conditions are present and the host
445 is under stress. Many *Colletotrichum* species are latent plant pathogens that remain asymptomatic
446 until conditions become conducive (Guarnaccia et al. 2017; Crous et al. 2016; De Silva et al. 2017;
447 Zaitlin et al. 2000). Moreover, latent infections can play a significant role in anthracnose diseases,
448 for example, serving as an inoculum source (Moral et al. 2009). More studies are needed to

449 determine the importance of latent infections on leaves and shoots in the *Colletotrichum* dieback
450 of citrus.

451 Several morphological characteristics have been used historically to identify *Colletotrichum*
452 species (Hyde et al. 2009; Sutton 1992). Conidium size was used in traditional identifications
453 systems and remains as part of the polyphasic approach proposed for taxonomic studies on
454 *Colletotrichum* (Cai et al. 2009). This characteristic has been used to differentiate morphotypes
455 correctly before molecular identification at the species level (Munir et al. 2016). In this work, the
456 conidium size showed differences between the species and was helpful to classify them. The
457 *Colletotrichum* species also differed in the number of conidia produced on PDA. The importance
458 of this characteristic for the identification of *Colletotrichum* species is limited, although has been
459 used in fitness comparison studies (Moral et al. 2021; Forcelini et al. 2018). Relative growth rates
460 in culture media can be used also to distinguish *Colletotrichum* species (Cai et al. 2009; Sutton
461 1992; Velho et al. 2015). Previous works indicated that species in the *C. gloeosporioides* species
462 complex had a higher growth rate than other *Colletotrichum* species infecting the same crop
463 (Munir et al. 2016). Our results demonstrated that *C. gloeosporioides* grow relatively faster than
464 *C. karstii* when compared at 25 °C. This difference in growth rate between these *Colletotrichum*
465 species was previously observed for isolates causing anthracnose of citrus in Australia (Wang et
466 al. 2021).

467 Phylogenetic analysis confirmed that the *Colletotrichum* isolates remaining as latent infections
468 on non-symptomatic twigs and leaves belong to *C. gloeosporioides* and *C. karstii*, as reported in
469 previous taxonomical studies on symptomatic tissues (Mayorquin et al. 2019; Riolo et al. 2021).
470 Moreover, the *Colletotrichum* isolates obtained in this study clustered together with isolates
471 obtained from these symptomatic tissues (Mayorquin et al. 2019), confirming that these pathogens
472 remain as latent infections on leaves and shoots, as observed in the survey. A clear and highly
473 supported separation of species was obtained by analyzing the genes included in this study. This
474 finding supports GAPDH and TUB2 as highly variable genes for differentiation at species levels
475 in the *C. gloeosporioides* and *C. karstii* species complexes, as suggested by Vieira et al. (2020).
476 The phylogenetic analysis also supported the classification of fungal isolates made based on
477 published descriptions. Other *Colletotrichum* species causing the same disease have been

478 separated according to morphological characteristics (Moral et al. 2021). Given the low number
479 of species causing *Colletotrichum* dieback in California citrus, this criterion could be relevant.

480 The response of physiological variables to different temperatures is a criterion commonly used
481 to characterize *Colletotrichum* species (López-Moral et al. 2017; Kenny et al. 2012; Pardo-De la
482 Hoz et al. 2016; Han et al. 2016). The optimum growth temperature did not differ between the
483 *Colletotrichum* species. The growth patterns obtained for the isolates included in this work were
484 similar to those described for other *Colletotrichum* species causing anthracnose in almonds
485 (López-Moral et al. 2017). In addition, authors working with isolates from citrus reported that *C.*
486 *gloeosporioides* and *C. karstii* grew faster at 25°C with than 30 and 35°C (Riolo et al. 2021). This
487 is in accordance with the results observed in our study. In other *Colletotrichum* diseases, isolates
488 of *C. gloeosporioides* showed optimal growth temperatures between 25-31 °C, while isolates of
489 *C. karstii* showed the highest growth rate at 25 °C (Kenny et al. 2012; Velho et al. 2015).
490 According to the Analytis Beta Model, the growth rates at the optimum temperature showed higher
491 values for *C. gloeosporioides* than *C. karstii*, confirming the results observed at 25°C. The
492 temperature also influenced conidial germination and appressorium formation. For *C.*
493 *gloeosporioides*, conidial germination increased with temperature, while appressorium formation
494 showed the opposite trend. These results did not coincide with those reported by Lima et al. (2011),
495 who worked with isolates causing PFD in citrus. For both processes, these authors indicated an
496 optimal temperature of approximately 25°C, with minimum and maximum temperatures of
497 roughly 6 and 40°C, respectively (Lima et al. 2011). Conversely, this description seems to match
498 the pattern observed for *C. karstii*, considering that lower conidial germination and appressorium
499 formation rates were observed at 10 and 35 °C. Temperature and wetness duration are critical
500 parameters that influence infection in *Colletotrichum* pathosystems (Diéguez-Uribeondo et al.
501 2011; Moral et al. 2012; Leandro et al. 2003). Recently, a conidium germination model has been
502 recommended to time fungicide applications to control PFD caused by *C. acutatum* and *C.*
503 *gloeosporioides* in citrus (Gama et al. 2019). Based on our results, the *Colletotrichum* species
504 causing dieback in California citrus differ in temperature requirements for conidial germination
505 and appressorium formation and this dissimilarity should be considered to validate this model.

506 Our results showed that *C. karstii* is more frequent than *C. gloeosporioides*, which is consistent
507 with previous studies performed in California but contrasts with reports from China, Italy, and

508 Portugal (Mayorquin et al. 2019; Riolo et al. 2021; Ramos et al. 2016; Huang et al. 2013). The
509 dominance of *C. karstii* over *C. gloeosporioides* could be related to the higher germination and
510 appressorium formation rates, as observed in this study.

511 Pathogenicity tests on citrus trees demonstrated the ability of *C. gloeosporioides* and *C. karstii*
512 to cause lesions on twigs. First studies on *Colletotrichum* dieback of citrus in California indicated
513 that *C. karstii* was a more aggressive pathogen than *C. gloeosporioides* based on experiments
514 under greenhouse conditions (Mayorquin et al. 2019). Conversely, in-field tests performed in Italy
515 determined that *C. gloeosporioides* was more aggressive than *C. karstii* on citrus twigs (Riolo et
516 al. 2021). Other studies also indicated that *C. gloeosporioides* causes lesions with a higher diameter
517 than those produced by *C. karstii* when inoculated on citrus fruits (Aiello et al. 2015; Guarnaccia
518 et al. 2017). Our study compared a significantly higher number of isolates than these previous
519 studies and no differences in aggressiveness were observed between the *Colletotrichum* species.
520 Other authors suggested that this discrepancy may be due, at least partially, to differences in
521 pathogenicity among isolates of the same species (Riolo et al. 2021). Isolates of *C. gloeosporioides*
522 associated with anthracnose in olive have been characterized by high variability in terms of
523 aggressiveness (Scheda et al. 2014; Moral et al. 2021). Because no intraspecific variability was
524 observed among the isolates included in our study, more experiments are needed to explain
525 dissimilar reports on the pathogenicity of pathogens that cause *Colletotrichum* dieback of citrus.

526 Several chemical classes are recommended in spray guides for *Colletotrichum* control on fruit
527 crops in the United States (Beckerman et al. 2022; Diepenbrock et al. 2020; Grafton-Cardwell et
528 al. 2021). However, no fungicide products are currently registered to control *Colletotrichum*
529 dieback of citrus in California. The fungicide screening performed in this study determined that
530 the DMI fungicides were the most effective in reducing the mycelial growth of *C. gloeosporioides*
531 and *C. karstii*. Gama et al. (2021) demonstrated that the mycelial growth of citrus *C. acutatum*
532 isolates were highly sensitive to DMI fungicides. The high efficacy of this chemical class against
533 *Colletotrichum* pathogens has also been documented in other pathosystems (Moral et al. 2018;
534 Chen et al. 2016). Moreover, metconazole and tebuconazole were indicated as effective fungicides
535 against pathogens of the *C. acutatum* and *C. gloeosporioides* species complexes isolated from
536 peach (Chen et al. 2016). Some fungicides that belong to the SDHI chemical class have shown
537 good efficacy in controlling *Colletotrichum* diseases based on results from field trials (Beckerman

538 et al. 2022). In California, some fungicide mixtures containing SDHI compounds are
539 recommended to control *C. gloeosporioides* causing anthracnose on citrus fruits (Grafton-
540 Cardwell et al. 2021; Mertely et al. 2018, 2019). Based on our results, the SDHI-fungicide
541 fluopyram does not have activity against the pathogens studied. This finding is in accordance with
542 Ishii et al. (2016) who indicated that *C. gloeosporioides* and *C. acutatum* isolates are naturally
543 tolerant to this active ingredient. Conversely, penthiopyrad caused fungal growth inhibition on the
544 studied pathogens when exposed to this SDHI-fungicide. The good performance of this active
545 ingredient among SDHI fungicides was previously reported by Ishii et al. (2016), who tested the
546 efficacy of penthiopyrad to inhibit mycelial growth of *Colletotrichum* species, including *C.*
547 *gloeosporioides*. Further studies proved the high inhibitory activity of penthiopyrad on the
548 mycelial growth of *C. gloeosporioides*, highlighting its potential to control *Colletotrichum*
549 diseases (Liang et al. 2020; Oliveira et al. 2020). In general, multisite protectant fungicides provide
550 moderate to good control of *Colletotrichum* diseases (Dowling et al. 2020). In our study, the
551 multisite fungicides showed a relatively low inhibitory activity on the mycelial growth of *C.*
552 *gloeosporioides* and *C. karstii*. Regarding spore germination, the QoI fungicides showed a
553 remarkably inhibitory effect on this process. It is considered that QoI fungicides are the most
554 effective chemical class against *Colletotrichum* spp., although this high efficacy has led to multiple
555 applications that resulted in the emergence of fungicide resistance (Forcelini et al. 2016; Dowling
556 et al. 2020). Present data from spore germination assays indicate no resistance to QoI fungicides
557 in citrus isolates of *C. gloeosporioides* and *C. karstii*. Furthermore, none of the SDHI fungicides
558 strongly inhibited conidial germination. The lack of efficacy to inhibit germination of conidia has
559 been previously reported for SDHI fungicides, including penthiopyrad (Ishii et al. 2016; Liang et
560 al. 2020).

561 On average, isolates of *C. karstii* were more sensitive to the DMI fungicides and chlorothalonil
562 than *C. gloeosporioides*. To our knowledge, this is the first study comparing the sensitivity of these
563 species, or their respective species complex, to these active ingredients. Limited information is
564 available in the literature regarding the fungicide sensitivity of *C. karstii*. Aiello et al. (2015)
565 indicated no differences between *C. karstii* and *C. gloeosporioides* regarding their sensitivity to
566 benomyl. In contrast, several previous studies highlighted differences in fungicide sensitivity
567 between *C. gloeosporioides* and *C. acutatum* species complexes (Munir et al. 2016; Cao et al.
568 2017; Peres et al. 2003). Munir et al. (2016) also reported differences in fungicide sensitivity

569 among species that belong to these complexes. A recent study using species of the *C. acutatum*
570 species complex related DMI fungicide sensitivity with CYP51 gene paralogs (Chen et al. 2020).
571 Future studies are required to determine the mechanisms conferring differential sensitivities to
572 fungicides.

573 The findings of this study provide new information about the pathogens that cause
574 *Colletotrichum* dieback in California citrus groves. Several epidemiological traits have been
575 addressed to understand this new pathosystem better. In this sense, we demonstrated that *C.*
576 *gloeosporioides* and *C. karstii* remain as latent infections on twigs and leaves. This information is
577 relevant since disease development can occur from latent infections when conditions become
578 conducive. The morphological and physiological descriptions provided in this study could be used
579 to accurately classify the pathogens. Differences in sensitivity to fungicides were found between
580 the *Colletotrichum* species. This finding highlights the importance of pathogen identification for
581 the successful management of the disease. The effective fungicide products reported in this study
582 should be considered for fungicide efficacy field trials and further included in an integrated pest
583 management strategy to mitigate *Colletotrichum* dieback in California citrus.

584 LITERATURE CITED

- 585 Adaskaveg, J. E., and Michailides, T. J. 2021. Fungicides, bactericides, and biologicals for
586 deciduous tree fruit, nut, citrus, strawberry, and vine crops. Online publication. [https://cfn-](https://cfn-fungicides.ucr.edu)
587 [fungicides.ucr.edu](https://cfn-fungicides.ucr.edu)
- 588 Adaskaveg, J. E., Forster, H., and Mauk, P. A. 2014. Fungal Diseases. In *Citrus Production*
589 *Manual*, eds. L. Ferguson and E. E. Grafton-Cardwell. Richmond, CA: University of
590 California, p. 307–326.
- 591 Aiello, D., Carrieri, R., Guarnaccia, V., Vitale, A., Lahoz, E., and Polizzi, G. 2015.
592 Characterization and pathogenicity of *Colletotrichum gloeosporioides* and *C. karstii* causing
593 preharvest disease on *Citrus sinensis* in Italy. *J. Phytopathol.* 163:168–177.
- 594 Beckerman, J. ., Bessin, R. ., Strang, J. ., Welty, C. ., Rodriguez-Salamanca, L. ., Athey, K. .,
595 Meyer, S. ., Long, E. ., Heller-Haas, M. ., Lewis-Ivey, M. ., Lewis, D. ., Guedot, C. ., Wahle,
596 E. ., Tucker, T. ., Wright, S. ., Becker, D. ., Hannan, J. ., Smigell, C. ., Onofre, R. ., et al. 2021.
597 Midwest Fruit Pest Management Guide 2021 - 2022. Online publication.
598 <https://ag.purdue.edu/hla/hort/documents/id-465.pdf>
- 599 Cai, L., Hyde, K. D., Taylor, P. W. J., Abang, M. M., Yang, Y. L., Liu, Z. Y., Shivas, R. G., 10,
600 Mckenzie, E. H. C., Johnston, Abang, J., Yang, J. Z., Liu, S., Shivas, Z. Y., Mckenzie, R. G.,
601 and Johnston, E. H. C. 2009. A polyphasic approach for studying *Colletotrichum*. *Fungal*
602 *Divers.* 39: 183-204.
- 603 Cannon, P. F., Damm, U., Johnston, P. R., and Weir, B. S. 2012. *Colletotrichum* - current status
604 and future directions. *Stud. Mycol.* 73:181–213.
- 605 Cao, X., Xu, X., Che, H., West, J. S., and Luo, D. 2017. Distribution and fungicide sensitivity of

- 606 Colletotrichum species complexes from Rubber Tree in Hainan, China. *Plant Dis.* 101:1774–
607 1780.
- 608 Chen, S., Hu, M., Schnabel, G., Yang, D., Yan, X., and Yuan, H. 2020. Paralogous CYP51 genes
609 of *Colletotrichum* spp. mediate differential sensitivity to sterol demethylation inhibitors.
610 *Phytopathology* 110: 615-625.
- 611 Chen, S. N., Luo, C. X., Hu, M. J., and Schnabel, G. 2016. Sensitivity of *Colletotrichum* species,
612 including *C. fioriniae* and *C. nymphaeae*, from peach to demethylation inhibitor fungicides.
613 *Plant Dis.* 100:2434–2441.
- 614 CIMIS. 2021. California Irrigation Management Information System (CIMIS). Available at
615 <https://cimis.water.ca.gov/>.
- 616 Crous, P. W., Groenewald, J. Z., Slippers, B., and Wingfield, M. J. 2016. Global food and fibre
617 security threatened by current inefficiencies in fungal identification. *Phil. Trans. R. Soc. B.*
618 371:20160024.
- 619 Damm, U., Cannon, P. F., Woudenberg, J. H. C., and Crous, P. W. 2012a. The *Colletotrichum*
620 *acutatum* species complex. *Stud. Mycol.* 73:37–113.
- 621 Damm, U., Cannon, P. F., Woudenberg, J. H. C., Johnston, P. R., Weir, B. S., Tan, Y. P., Shivas,
622 R. G., and Crous, P. W. 2012b. The *Colletotrichum boninense* species complex. *Stud. Mycol.*
623 73:1–36.
- 624 Diéguez-Uribeondo, J., Förster, H., and Adaskaveg, J. E. 2011. Effect of wetness duration and
625 temperature on the development of anthracnose on selected almond tissues and comparison
626 of cultivar susceptibility. *Phytopathology.* 101:1013–1020.
- 627 Diepenbrock, L. M., Dewdney, M. M., Vashisth, T., Kanissery, R., and Futch, S. H. 2020. 2020–
628 2021 Florida Citrus Production Guide: Pesticides Registered for Use on Florida Citrus.
629 Department of Entomology and Nematology, UF/IFAS Extension. Online publication.
630 doi.org/10.32473/edis-cg101-2021
- 631 Dowling, M., Peres, N., Villani, S., and Schnabel, G. 2020. Managing *Colletotrichum* on fruit
632 crops: a “complex” challenge. *Plant Dis.* 104:2301–2316.
- 633 Forcelini, B. B., Rebello, C. S., Wang, N., and Peres, N. A. 2018. Fitness, competitive ability, and
634 mutation stability of isolates of *Colletotrichum acutatum* from strawberry resistant to QoI
635 fungicides. *Phytopathology* 108:462–468.
- 636 Forcelini, B. B., Seijo, T. E., and Peres, N. A. 2016. Resistance in strawberry isolates of
637 *Colletotrichum acutatum* from Florida to quinone-oxidoreductase inhibitor fungicides. *Plant Dis.*
638 100:2050-2056
- 639 Förster, H., Kanetis, L., and Adaskaveg, J. E. 2004. Spiral gradient dilution, a rapid method for
640 determining growth responses and 50% effective concentration values in fungus-fungicide
641 interactions. *Phytopathology* 94 (2): 163-170.
- 642 Gama, A. B., Baggio, J. S., Rebello, C. S., de Afonseca Lourenço, S., de Gasparoto, C. G., José da
643 Silva Junior, G., Peres, N. A., and Amorim, L. 2021. Sensitivity of *Colletotrichum acutatum*
644 isolates from citrus to carbendazim, difenoconazole, tebuconazole, and trifloxystrobin. *Plant*
645 *Dis.* 104:1621-1628.
- 646 Gama, A. B., Silva Junior, G. J., Peres, N. A., Edwards Molina, J., de Lima, L. M., and Amorim,
647 L. 2019. A threshold-based decision-support system for fungicide applications provides cost-
648 effective control of citrus postbloom fruit drop. *Plant Dis.* 103:2433–2442.
- 649 Grafton-Cardwell, E. E., Baldwin, R. A., Becker, J. O., Eskalen, A., Lovatt, C. J., Rios, S.,
650 Adaskaveg, J. E., Faber, B. A., Haviland, D. R., Hembree, K. J., Morse, J. G., and Westerdahl,
651 B. B. 2021. UC IPM pest management guidelines: citrus. UC ANR Publication 3441.

- 652 Oakland, CA.
- 653 Guarnaccia, V., Groenewald, J. Z., Polizzi, G., and Crous, P. W. 2017. High species diversity in
654 *Colletotrichum* associated with citrus diseases in Europe. *Persoonia - Mol. Phylogeny Evol.*
655 *Fungi.* 39:32–50.
- 656 Guerber, J. C., Liu, B., Correll, J. C., and Johnston, P. R. 2003. Characterization of diversity in
657 *Colletotrichum acutatum sensu lato* by sequence analysis of two gene introns, mtDNA and
658 intron RFLPs, and mating compatibility. *Mycologia.* 95:872–895.
- 659 Han, Y. C., Zeng, X. G., Xiang, F. Y., Chen, F. Y., and Gu, Y. C. 2016. Distribution and
660 characteristics of *Colletotrichum* spp. associated with anthracnose of strawberry in Hubei,
661 China. *Plant Dis.* 100:996-1006.
- 662 Huang, F., Chen, G. Q., Hou, X., Fu, Y. S., Cai, L., Hyde, K. D., and Li, H. Y. 2013. *Colletotrichum*
663 species associated with cultivated citrus in China. *Fungal Divers.* 61:61–74.
- 664 Hyde, K. D., Cai, L., Mckenzie, E. H. C., Yang, Y. L., Zhang, J. Z., Prihastuti, H., and Prihastuti,
665 J. Z. 2009. *Colletotrichum*: a catalogue of confusion. *Fungal Diversity* 39: 1-17.
- 666 Ishii, H., Zhen, F., Hu, M., Li, X., and Schnabel, G. 2016. Efficacy of SDHI fungicides, including
667 benzovindiflupyr, against *Colletotrichum* species. *Pest Manag. Sci.* 72:1844–1853.
- 668 Kalyanamorthy, S., Minh, B.Q., Wong, T.K.F., von Haeseler, A., Jermini, L.S., 2017.
669 ModelFinder: fast model selection for accurate phylogenetic estimates. *Nat. Met.* 14, 587–
670 589.
- 671 Katoh, K., Standley, D.M., 2013. MAFFT Multiple Sequence Alignment Software Version 7:
672 improvements in performance and usability. *Mol. Biol. Evol.* 30, 772–780.
- 673 Kenny, M. K., Galea, V. J., and Price, T. V. 2012. Germination and growth of *Colletotrichum*
674 *acutatum* and *Colletotrichum gloeosporioides* isolates from coffee in Papua New Guinea and
675 their pathogenicity to coffee berries. *Australas. Plant Pathol.* 41:519–528.
- 676 Kumar, S., Stecher, G., Tamura, K., 2016. MEGA7: Molecular evolutionary genetics analysis
677 version 7.0 for bigger datasets. *Mol. Biol. Evol.* 33, 1870–1874.
- 678 Leandro, L. F. S., Gleason, M. L., Nutter, F. W., Wegulo, S. N., and Dixon, P. M. 2003. Influence
679 of temperature and wetness duration on conidia and appressoria of *Colletotrichum acutatum*
680 on symptomless strawberry leaves. *Phytopathology* 93:513-520.
- 681 Liang, X., Peng, Y., Zou, L., Wang, M., Yang, Y., and Zhang, Y. 2020. Baseline sensitivity of
682 penthiopyrad against *Colletotrichum gloeosporioides* species complex and its efficacy for the
683 control of *Colletotrichum* leaf disease in rubber tree. *Eur. J. Plant Pathol.* 158:965–974.
- 684 Lima, W. G., Spósito, M. B., Amorim, L., Gonçalves, F. P., and de Filho, P. A. M. 2011.
685 *Colletotrichum gloeosporioides*, a new causal agent of citrus post-bloom fruit drop. *Eur. J.*
686 *Plant Pathol.* 131:157–165.
- 687 López-Moral, A., Raya-Ortega, M. C., Agustí-Brisach, C., and Roca, L. F. 2017. Morphological,
688 pathogenic, and molecular characterization of *Colletotrichum acutatum* isolates causing
689 almond anthracnose in Spain. *Plant Dis.* 101:2034-2045.
- 690 Lovatt, C. J. 2014. Physiology and Phenology. In *Citrus Production Manual*, eds. L. Ferguson and
691 L. F. Grafton-Cardwell. University of California, USA.
- 692 Mayorquin, J. S., Nouri, M. T., Peacock, B. B., Trouillas, F. P., Douhan, G. W., Kallsen, C., and
693 Eskalen, A. 2019. Identification, pathogenicity, and spore trapping of *Colletotrichum karstii*
694 associated with twig and shoot dieback in California. *Plant Dis.* 103:1464–1473.
- 695 Marin-Felix Y, Groenewald JZ, Cai L, et al. (2017). Genera of phytopathogenic fungi: GOPHY 1.
696 *Stud. Mycol.* 86:99–216.
- 697 Mertely, J. C., Seijo, T., and Peres, N. 2019. Evaluation of products and programs for anthracnose

- 698 fruit rot in annual strawberry, 2018-2019. *Plant Dis. Manag. Rep.* 8:SMF013.
- 699 Mertely, J., Seijo, T., and Peres, N. A. 2018. Evaluation of products for anthracnose fruit rot and
700 *Gnomonia* leaf blotch control in strawberry, 2016- 2017. *Plant Dis. Manag. Rep.* 12:PF046.
- 701 Moral, J., Agustí-Brisach, C., Raya, M. C., Jurado- Bello, J., López-Moral, A., Roca, L. F.,
702 Chattaoui, M., Rhouma, A., Nigro, F., Sergeeva, V., and Trapero, A. 2021. Diversity of
703 *Colletotrichum* species associated with olive anthracnose worldwide. *Journal of Fungi*, 7(9),
704 741.
- 705 Moral, J., Agustí-Brisach, C., Agalliu, G., de Oliveira, R., Pérez-Rodríguez, M., Roca, L. F.,
706 Romero, J., and Trapero, A. 2018. Preliminary selection and evaluation of fungicides and
707 natural compounds to control olive anthracnose caused by *Colletotrichum* species. *Crop Prot.*
708 114:167–176.
- 709 Moral, J., Jurado-Bello, J., Sánchez, M. I., De Oliveira, R., and Trapero, A. 2012. Effect of
710 temperature, wetness duration, and planting density on olive anthracnose caused by
711 *Colletotrichum* spp. *Phytopathology*. 102:974–981.
- 712 Moral, J., De Oliveira, R., and Trapero, A. 2009. Elucidation of the disease cycle of olive
713 anthracnose caused by *Colletotrichum acutatum*. *Phytopathology* 99:548-556.
- 714 Munir, M., Amsden, B., Dixon, E., Vaillancourt, L., and Gauthier, N. A. W. 2016. Characterization
715 of *Colletotrichum* species causing bitter rot of apple in Kentucky orchards. *Plant Dis.*
716 100:2194-2203.
- 717 Oliveira, M. S., Cordova, L. G., and Peres, N. A. 2020. Efficacy and baseline sensitivity of
718 succinate-dehydrogenase-inhibitor fungicides for management of *Colletotrichum* crown rot
719 of strawberry. *Plant Dis.* 104:2860–2865.
- 720 Pardo-De la Hoz, C. J., Calderón, C., Rincón, A. M., Cárdenas, M., Danies, G., López-Kleine, L.,
721 Restrepo, S., and Jiménez, P. 2016. Species from the *Colletotrichum acutatum* ,
722 *Colletotrichum boninense* and *Colletotrichum gloeosporioides* species complexes associated
723 with tree tomato and mango crops in Colombia. *Plant Pathol.* 65:227–237.
- 724 Peres, N. A., Souza, N. L., Peever, T. L., and Timmer, L. W. 2003. Benomyl sensitivity of isolates
725 of *Colletotrichum acutatum* and *C. gloeosporioides* from Citrus. *Plant Dis.* 88:125–130.
- 726 Piccirillo, G., Carrieri, R., Polizzi, G., Azzaro, A., Lahoz, E., Fernández-Ortuño, D., and Vitale,
727 A. 2018. In vitro and in vivo activity of QoI fungicides against *Colletotrichum*
728 *gloeosporioides* causing fruit anthracnose in *Citrus sinensis*. *Sci. Hortic.* 236:30–95.
- 729 Pryor, B. M., and Michailides, T. J. 2002. Morphological, pathogenic, and molecular
730 characterization of *Alternaria* isolates associated with *Alternaria* late blight of pistachio.
731 *Phytopathology*. 94:406–416.
- 732 Ramos, A. P., Talhinhos, P., Sreenivasaprasad, S., and Oliveira, H. 2016. Characterization of
733 *Colletotrichum gloeosporioides*, as the main causal agent of citrus anthracnose, and *C. karstii*
734 as species preferentially associated with lemon twig dieback in Portugal. *Phytoparasitica*
735 44:549–561.
- 736 Riolo, M., Aloi, F., Pane, A., Cara, M., and Cacciola, S. O. 2021. Twig and shoot dieback of citrus,
737 a new disease caused by *Colletotrichum* species. *Cells* 10(2):449.
- 738 Schena, L., Mosca, S., Cacciola, S. O., Faedda, R., Sanzani, S. M., Agosteo, G. E., Sergeeva, V.,
739 Magnano Di, G., and Lio, S. 2014. Species of the *Colletotrichum gloeosporioides* and *C.*
740 *boninense* complexes associated with olive anthracnose. *Plant Pathol.* 63:437–446.
- 741 De Silva, D. D., Crous, P. W., Ades, P. K., Hyde, K. D., and Taylor, P. W. J. 2017. Life styles of
742 *Colletotrichum* species and implications for plant biosecurity. *Fungal Biol. Rev.* 31:155–168.
- 743 Smith, B. J. 2008. Epidemiology and pathology of strawberry anthracnose: A north american

- 744 perspective. Hort. Science. 13:69-73.
- 745 Sutton, B. C. 1992. The genus *Glomerella* and its anamorph *Colletotrichum*. Pages 1-26 in:
746 *Colletotrichum—Biology, Pathology, and Control*. J. A. Bailey and M. J. Jeger, eds. CAB
747 International, Wallingford, United Kingdom.
- 748 Takele, E. 2014. Cost of Establishment and Production. In *Citrus Production Manual*, eds. L.
749 Ferguson and E. E. Grafton-Cardwell. University of California, USA.
- 750 Timmer, L. W., Agostini, J. P., Zitko, S. E., and Zulfikar, M. 1994. Postbloom fruit drop, an
751 increasingly prevalent disease of citrus in the Americas. *Plant Dis.* 78:329–334.
- 752 Torres-Londoño, A., Hausbeck, G., Hausbeck, M., and Jianjun, H. 2016. ECX: An R Package for
753 Studying Sensitivity of Antimicrobial Substances Using Spiral Plating Technology. *Plant*
754 *Heal. Prog.* 17:188–194.
- 755 United States Department of Agriculture-National Agricultural Statistics Service. 2020. Citrus
756 Fruits: 2020 Summary, August 2020. USDA-NASS. Online publication.
757 https://www.nass.usda.gov/Publications/Todays_Reports/reports/cftr0820.pdf
- 758 Velho, A. C., Alaniz, S., Casanova, L., Mondino, P., Stadnik, M. J., and Schoch, C. 2015. New
759 insights into the characterization of *Colletotrichum* species associated with apple diseases in
760 southern Brazil and Uruguay. *Fungal Biol.* 119:229-244.
- 761 Vieira, W. A. d. S., Alves Bezerra, P., Carlos Da Silva, A., Veloso, S., Paz, M., Câmara, S., and
762 Patrick Doyle, V. 2020. Optimal markers for the identification of *Colletotrichum* species.
763 *Mol. Phylogenet. Evol.* 143:106694.
- 764 Wang, W., de Silva, D. D., Moslemi, A., Edwards, J., Ades, P. K., Crous, P. W., and Taylor, P.
765 W. J. 2021. *Colletotrichum* species causing anthracnose of citrus in Australia. *J. Fungi.* 7: 47.
- 766 Weir, B. S., Johnston, P. R., and Damm, U. 2012. The *Colletotrichum gloeosporioides* species
767 complex. *Stud. Mycol.* 73:115–180.
- 768 White, T. J., Bruns, T., Lee, S., and Taylor, J. 1990. Academic Press, San Diego, CA. In *PCR*
769 *Protocols: A Guide to Methods and Applications.*, San Diego, CA: Academic Press.
- 770 Yang, X., Wilson, L. L., Madden, L. V., and Ellis, M. A. 1990. Rain splash dispersal of
771 *Colletotrichum acutatum* from infected strawberry fruit. *Phytopathology.* 80:590–595.
- 772 Zaitlin, B., Zehr, E. I., and Dean, R. A. 2000. Latent infection of peach caused by *Colletotrichum*
773 *gloeosporioides* and *Colletotrichum acutatum*. *Can. J. Plant Pathol.* 22: 224-228.
- 774 Zhang, D., Gao, F., Jakovlić, I., Zou, H., Zhang, J., Li, W.X., Wang, G.T., 2019. PhyloSuite: An
775 integrated and scalable desktop platform for streamlined molecular sequence data
776 management and evolutionary phylogenetics studies. *Mol. Ecol. Res.* 20(1): 348-355.

777 TABLE 1. Description of *Colletotrichum* spp. isolates used in the phylogenetic analysis and their
778 respective GenBank accession numbers.

Species ^a	Isolate ^b	Location	Host	Cultivar	GenBank accession number ^c		
					ITS	GAPDH	TUB2
<i>Colletotrichum gloeosporioides</i>	13I49	Tulare	<i>Citrus reticulata</i>	Clemenules	MZ571664	MZ574969	MZ558773
<i>C. gloeosporioides</i>	13I50	Tulare	<i>C. reticulata</i>	Clemenules	MZ571665	MZ574970	MZ558774
<i>C. gloeosporioides</i>	13I56	Tulare	<i>C. reticulata</i>	Tango	MZ571666	MZ574971	MZ558775
<i>C. gloeosporioides</i>	13J65	Tulare	<i>C. reticulata</i>	Tango	MZ571670	MZ574975	MZ558779
<i>C. gloeosporioides</i>	13J85	Tulare	<i>C. reticulata</i>	Tango	MZ571671	MZ574976	MZ558780
<i>C. gloeosporioides</i>	13G36	Fresno	<i>C. reticulata</i>	Tango	MZ571661	MZ574966	MZ558770
<i>C. gloeosporioides</i>	13I46	Tulare	<i>C. sinensis</i>	Atwood	MZ571663	MZ574968	MZ558772
<i>C. gloeosporioides</i>	13I57	Tulare	<i>C. sinensis</i>	Washington	MZ571667	MZ574972	MZ558776
<i>C. gloeosporioides</i>	13I58	Tulare	<i>C. sinensis</i>	Fukumoto	MZ571668	MZ574973	MZ558777
<i>C. gloeosporioides</i>	13J55	Tulare	<i>C. sinensis</i>	Washington	MZ571669	MZ574974	MZ558778
<i>C. gloeosporioides</i>	13I45	Tulare	<i>Citrus sinensis</i>	Atwood	MZ571662	MZ574967	MZ558771
<i>C. karstii</i>	13F53	Fresno	<i>C. reticulata</i>	Owari Satsuma	MZ571629	MZ574978	MZ542797
<i>C. karstii</i>	13I37	Tulare	<i>C. reticulata</i>	Sumo	MZ571630	MZ574979	MZ542798
<i>C. karstii</i>	13I47	Tulare	<i>C. reticulata</i>	Tango	MZ571631	MZ574980	MZ542799
<i>C. karstii</i>	13I51	Tulare	<i>C. reticulata</i>	Sumo	MZ571632	MZ574981	MZ542800
<i>C. karstii</i>	13J74	Fresno	<i>C. reticulata</i>	Clemenules	MZ571634	MZ574983	MZ542802
<i>C. karstii</i>	13J89	Fresno	<i>C. reticulata</i>	Clemenules	MZ571635	MZ574984	MZ542803
<i>C. karstii</i>	13I98	Tulare	<i>C. sinensis</i>	Washington	MZ571633	MZ574982	MZ542801
<i>C. karstii</i>	13F29	Fresno	<i>C. sinensis</i>	Cara-Cara	MZ571628	MZ574977	MZ542796
<i>C. aeshynomenes</i>	ICMP 17673*	USA	<i>Aeshynomene virginica</i>	...	JX010176	JX009930	JX010392
<i>C. alatae</i>	ICMP 17919*	India	<i>Dioscorea alata</i>	...	JX010190	JX009990	JX010383
<i>C. alienum</i>	ICMP 12071*	New Zealand	<i>Malus domestica</i>	...	JX010251	JX010028	JX010411
<i>C. annellatum</i>	CBS129826*	Colombia	<i>Hevea brasiliensis</i>	...	JQ005222	JQ005309	JQ005656
<i>C. aenigma</i>	ICMP 18608*	Israel	<i>Persea americana</i>	...	JX010244	JX010044	JX010389
<i>C. aenigma</i>	ICMP 18686	Japan	<i>Pyrus pyrifolia</i>	...	JX010243	JX003313	JX010390
<i>C. aotearoa</i>	ICMP 18537*	New Zealand	<i>Coprosma sp.</i>	...	JX010205	JX010005	JX010420
<i>C. asianum</i>	ICMP 18580*	Thailand	<i>Coffea arabica</i>	...	FJ972612	JX010053	JX010406
<i>C. boninense</i>	CBS128547	New Zealand	<i>Camellia sp.</i>	...	JQ005159	JQ005246	JQ005593
<i>C. boninense</i>	CBS123755*	Japan	<i>Crinum asiaticum var. sinicum</i>	...	JQ005153	JQ005240	JQ005588
<i>C. beeveri</i>	CBS128527*	New Zealand	<i>Brachyglottis repanda</i>	...	JQ005171	JQ005258	JQ005605
<i>C. brasiliense</i>	CBS128501	Brazil	<i>P. edulis</i>	...	JQ005235	JQ005322	JQ005669
<i>C. brassicicola</i>	CBS101059*	New Zealand	<i>Brassica oleracea var. gemmifera</i>	...	JQ005172	JQ005259	JQ005606
<i>C. camelliae-japonicae</i>	CGMCC 3.18118*	Japan	<i>Camellia japonica</i>	...	KX853165	KX893584	KX893580
<i>C. citricola</i>	CBS134228*	China	<i>Citrus unshiu</i>	...	KC293576	KC293736	KC293656
<i>C. changpingense</i>	MFLUCC 15-0022	China	<i>Fragaria × ananassa</i>	...	KP683152	KP852469	KP852490
<i>C. clidemiae</i>	ICMP 18658*	USA	<i>Clidemia hirta</i>	...	JX010265	JX009989	JX010438
<i>C. colombiense</i>	CBS129818*	Colombia	<i>P. edulis</i>	...	JQ005174	JQ005261	JQ005608
<i>C. conoide</i>	CGMCC 3.17615*	China	<i>Capsicum sp.</i>	...	KP890168	KP890162	KP890174
<i>C. constrictum</i>	CBS128504*	New Zealand	<i>Citrus limon</i>	...	JQ005238	JQ005325	JQ005672
<i>C. cordylinicola</i>	ICMP 18579*	Thailand	<i>Cordyline fruticosa</i>	...	JX010226	JX009975	JX010440
<i>C. cymbidiicola</i>	IMI 347923*	Australia	<i>Cymbidium sp.</i>	...	JQ005166	JQ005253	JQ005600
<i>C. dacrycarpi</i>	CBS130241*	New Zealand	<i>Dacrycarpus dacrydioides</i>	...	JQ005236	JQ005323	JQ005670
<i>C. endophytica</i>	MFLUCC 13-0418*	Thailand	<i>Pennisetum purpureum</i>	...	KC633854	KC832854	-
<i>C. fructicola</i>	ICMP 18581*	Thailand	<i>Coffea arabica</i>	...	JX010165	JX010033	JX010405
<i>C. fructicola</i>	ICMP 18646*	Panama	<i>Tetragastris panamensis</i>	...	JX010173	JX010032	JX010409
<i>C. fructivorum</i>	CBS 133125*	USA	<i>Vaccinium macrocarpon</i>	...	JX145145	-	JX145196
<i>C. grevilleae</i>	CBS 132879	Italy	<i>Grevillea sp.</i>	...	KC297078	KC297010	KC297102
<i>C. grossum</i>	CGMCC3.17614	China	<i>Capsicum sp.</i>	...	KP890165	KP890159	KP890171
<i>C. gloeosporioides</i>	CBS 273.51*	Italy	<i>Citrus limon</i>	...	JX010148	JX010054	-

Phytopathology
Camiletti et al. 2021

<i>C. gloeosporioides</i>	ICMP12938	New Zealand	<i>Citrus sinensis</i>	...	JX010147	JX009935	-
<i>C. gloeosporioides</i>	ICMP12939	New Zealand	<i>Citrus sp.</i>	...	JX010149	JX009931	-
<i>C. gloeosporioides</i>	ICMP118695	USA	<i>Citrus sp.</i>	...	JX010153	JX009979	-
<i>C. gloeosporioides</i>	ICMP18697	USA	<i>Vitis vinifera</i>	...	JX010154	JX009987	-
<i>C. gloeosporioides</i>	ICMP17821*	Italy	<i>Citrus sinensis</i>	...	JX010152	JX010056	-
<i>C. gloeosporioides</i>	KARE527	Fresno	<i>C. reticulata</i>	...	KY076552	KY304062	KY086322
<i>C. gloeosporioides</i>	KARE528	Fresno	<i>C. reticulata</i>	...	KY076553	KY304063	KY086323
<i>C. gloeosporioides</i>	KARE532	Fresno	<i>C. reticulata</i>	...	KY076554	KY304064	KY086324
<i>C. gloeosporioides</i>	KARE538	Fresno	<i>C. reticulata</i>	...	KY076556	KY304066	KY086326
<i>C. gloeosporioides</i>	KARE541	Fresno	<i>C. reticulata</i>	...	KY076558	KY304068	KY086328
<i>C. gloeosporioides</i>	KARE543	Fresno	<i>C. reticulata</i>	...	KY076559	KY304069	KY086329
<i>C. gloeosporioides</i>	KARE546	Fresno	<i>C. reticulata</i>	...	KY076560	KY304070	KY086330
<i>C. gloeosporioides</i>	KARE548	Fresno	<i>C. reticulata</i>	...	KY076561	KY304071	KY086331
<i>C. gloeosporioides</i>	UCR2575	Tulare	<i>C. reticulata</i>	4B	KY076567	KY304075	KY086335
<i>C. gloeosporioides</i>	KARE31	Solano	<i>C. sinensis</i>	...	KY076549	KY304060	KY086320
<i>C. gloeosporioides</i>	KARE37	Solano	<i>C. sinensis</i>	...	KY076551	KY304061	KY086321
<i>C. hebeiense</i>	MFLUCC13-0726*	China	<i>Vitis vinifera</i>	...	KF156863	KF377495	KF288975
<i>C. henanense</i>	CGMCC 3.17354*	China	<i>Camellia sp.</i>	...	KJ955109	KJ954810	KJ955257
<i>C. hippeastri</i>	CBS125376*	China	<i>H. vittatum</i>	...	JQ005231	JQ005318	JQ005665
<i>C. horii</i>	ICMP 10492*	Japan	<i>Diospyros kaki</i>	...	GQ329690	GQ329681	JX010450
<i>C. horii</i>	ICMP 17968	China	<i>Diospyros kaki</i>	...	JX010212	GQ329682	JX010378
<i>C. jiangxiense</i>	CGMCC 3.17363*	China	<i>Camellia sp.</i>	...	KJ955201	KJ954902	KJ955348
<i>C. kahawae subsp. ciggario</i>	ICMP 17922*	Australia	<i>Olea europaea</i>	...	JX010230	JX009966	JX010434
<i>C. karstii</i>	KARE523	Fresno	<i>C. reticulata</i>	...	KY076519	KY304041	KY086302
<i>C. karstii</i>	KARE524	Fresno	<i>C. reticulata</i>	...	KY076520	KY304042	KY086303
<i>C. karstii</i>	KARE525	Fresno	<i>C. reticulata</i>	...	KY076521	KY304043	KY086304
<i>C. karstii</i>	KARE526	Fresno	<i>C. reticulata</i>	...	KY076522	KY304044	KY086305
<i>C. karstii</i>	KARE530	Fresno	<i>C. reticulata</i>	...	KY076523	KY304045	KY086306
<i>C. karstii</i>	CBS 129833	Mexico	<i>Musa sp.</i>	...	JQ005175	JQ005262	JQ005609
<i>C. karstii</i>	CBS 129834	Mexico	<i>Musa sp.</i>	...	JQ005176	JQ005263	JQ005610
<i>C. karstii</i>	CBS 124969	Panama	<i>Quercus salicifolia</i>	...	JQ005179	JQ005266	JQ005613
<i>C. karstii</i>	CORCG6*	China	<i>Vanda sp.</i>	...	HM585409	HM585391	HM585428
<i>C. musae</i>	ICMP 17817	Kenya	<i>Musa sapientum</i>	...	JX010142	JX010015	JX010395
<i>C. musae</i>	ICMP 19119	USA	<i>Musa sp.</i>	...	JX010146	JX010050	HQ596280
<i>C. novae-zalandiae</i>	CBS 128505	New Zealand	<i>Capsicum annum</i>	...	JQ005228	JQ005315	JQ005662
<i>C. nupharicola</i>	ICMP 17938	USA	<i>Nuphar lutea</i>	...	JX010189	JX009936	JX010397
<i>C. nupharicola</i>	ICMP 18187	USA	<i>Nuphar lutea</i>	...	JX010187	JX009972	JX010398
<i>C. oncidii</i>	CBS 129828*	Germany	<i>Oncidium sp.</i>	...	JQ005169	JQ005256	JQ005603
<i>C. parsonsiiae</i>	CBS 128525	New Zealand	<i>Parsonsia capsularis</i>	...	JQ005233	JQ005320	JQ005667
<i>C. petchii</i>	CBS 378.94*	Italy	<i>Dracaena marginata</i>	...	JQ005223	JQ005310	JQ005657
<i>C. proteae</i>	CBS 132882	South Africa	<i>Protea sp.</i>	...	KC297079	KC297009	KC297101
<i>C. psidii</i>	ICMP 19120*	Italy	<i>Psidium sp.</i>	...	JX010219	JX009967	JX010443
<i>C. phyllanthi</i>	CBS175.67*	India	<i>Phyllanthus acidus</i>	...	JQ005221	JQ005308	JQ005655
<i>C. queenslandicum</i>	ICMP 1778*	Australia	<i>Carica papaya</i>	...	JX010276	JX009934	JX010398
<i>C. queenslandicum</i>	ICMP 18705	Fiji	<i>Coffea sp.</i>	...	JX010185	JX010036	JX010412
<i>C. rhexiae</i>	CBS 133134*	USA	<i>Rhexia virginica</i>	...	JX145128	-	JX145179
<i>C. salsolae</i>	ICMP 19051*	Hungary	<i>Salsola tragus</i>	...	JX010242	JX009916	JX010403
<i>C. siamense</i>	ICMP 17795	USA	<i>Malus domestica</i>	...	JX101162	JX010051	JX010393
<i>C. siamense</i>	ICMP 18578	Thailand	<i>Coffea arabica</i>	...	JX010171	JX009924	JX010404
<i>C. temperatum</i>	CBS 133122*	USA	<i>Vaccinium macrocarpon</i>	...	JX145159	-	JX145211
<i>C. ti</i>	ICMP 4832*	New Zealand	<i>Cordyline sp.</i>	...	JX010269	JX009952	JX010442
<i>C. theobromicola</i>	ICMP 18649*	Panama	<i>Theobroma cacao</i>	...	JX010294	JX010006	JX010447
<i>C. torulosum</i>	CBS128544*	New Zealand	<i>Solanum melongena</i>	...	JQ005164	JQ005251	JQ005598
<i>C. tropicale</i>	ICMP18653*	Panama	<i>Theobroma cacao</i>	...	JX010264	JX010007	JX010407
<i>C. viniferum</i>	GZAAS 5.08601	China	<i>Vitis vinifera</i>	...	JN412804	JN412798	JN412813
<i>C. wuxiense</i>	CGMCC 3.17894*	China	<i>Camellia sinensis</i>	...	KU251591	KU252045	KU252200
<i>C. xanthorrhoeae</i>	ICMP 17903*	Australia	<i>Xanthorrhoea sp.</i>	...	JX010261	JX009927	JX010448
<i>Colletotrichum sp.</i>	CBS123921	Japan	<i>Dendrobium kingianum</i>	...	JQ005163	JQ005250	JQ005597

<i>G. cingulata f.sp. camelliae</i>	ICMP 10646	USA	<i>Camellia sasanqua</i>	...	JX010225	JX009993	JX010437
-------------------------------------	------------	-----	--------------------------	-----	----------	----------	----------

779 ^x Species in bold indicate sequences from GenBank used in the phylogenetic analysis.

780 ^y CBS = Culture collection of the Centraalbureau Voor Schimmelcultures, Fungal Biodiversity
 781 Centre, Utrecht, The Netherlands; CGMCC = Chinese General Microbiological Culture Collection
 782 Center, Beijing, China; CORC = unknown; GZAAS = Guizhou Academy of Agricultural Sciences,
 783 Guizhou Province, China; ICMP = International Collection of Microorganisms from Plants,
 784 Auckland, New Zealand; IMI = International Mycological Institute, Kew, UK; KARE = Kearney
 785 Agricultural Research and Extension Center, Parlier, CA; MFLUCC = Mae Fah Luang University
 786 Culture Collection, Chiang Ria, Thailand; UCR = University of California, Riverside. An asterisk
 787 (*) denotes type/ex-type material.

788 ^z ITS = internal transcribed spacer; GAPDH = glyceraldehyde-3-phosphate dehydrogenase; TUB2
 789 = beta-tubulin.

790

791 TABLE 2. Fungicides used in sensitivity assays.

Active ingredient (%)	Manufacturer	Trade name	Formulation ^a	FRAC ^b group	Group name ^c
Azoxystrobin (22.9)	Syngenta	Abound	F	11	QoI
Trifloxystrobin (42.6)	Bayer	Gem 500	SC	11	QoI
Fluopyram (40.9)	Bayer	Luna Privilege	SC	7	SDHI
Penthiopyrad (20.4)	DuPont	Fontelis	SC	7	SDHI
Metconazole (50.0)	Valent	Quash	WDG	3	DMI
Tebuconazole (38.7)	Bayer	Folicur	F	3	DMI
Chlorothalonil (54.0)	Syngenta	Bravo	SC	M05	Chloronitriles
Cu hydroxide (46.1)	Certis	Kocide-3000	DF	M01	Inorganic

792 ^a F=flowable; SC= suspension concentrate; WDG= water dispersible granule; DF= Dry flowable.793 ^b FRAC= Fungicide resistance action committee.794 ^c QoI= Quinone outside Inhibitors; SDHI= Succinate-dehydrogenase inhibitors; DMI=
795 DeMethylation Inhibitors.

796

797 TABLE 3. Conidial production and dimensions of *C. gloeosporioides* (n=15) and *C. karstii* (n=15)
798 isolates infecting citrus twigs and leaves.

Morphological group	Sporulation rate ($\times 10^5/\text{cm}^2$) ^a	Conidium size		
		Length (μm) ^a	Width (μm) ^a	Volume (μm^3) ^a
<i>C. gloeosporioides</i>	1.79 \pm 0.54 a	15.8 \pm 1.52 a	6.8 \pm 0.84 b	577 \pm 157 b
<i>C. karstii</i>	1.50 \pm 0.92 b	14.5 \pm 1.42 b	7.8 \pm 0.91 a	702 \pm 194 a

799 ^a For each variable, the measure represents the mean value obtained from 15 isolates \pm standard
800 deviation. Means followed by different letters within a column are significantly different according
801 to Kruskal-Wallis all pairwise comparisons test ($P=0.05$).

802

803 TABLE 4. Temperature-growth relationship for *Colletotrichum karstii* and *C. gloeosporioides*
804 representative isolates.

Species	Isolate	Analytis Beta Model ^x			Temperature (°C)			MGR (mm day ⁻¹) ^z		
		<i>d</i>	<i>a</i>	<i>b</i>	Minimum	Maximum	Optimum ^y			
<i>C. karstii</i>										
	13F29	4.4x10 ⁻⁰⁷	3.31	1.91	5	35	24.0	a	8.1	a
	13J89	6.9x10 ⁻⁰⁷	3.17	1.76	3	35	23.6	a	8.0	a
	13J74	4.9x10 ⁻⁰⁶	2.79	1.53	4	35	24.0	a	8.2	a
<i>C. gloeosporioides</i>										
	13J85	4.9x10 ⁻⁰⁴	1.65	1.1	7	35	23.8	a	10.3	a
	13I46	5.4x10 ⁻⁰⁴	1.37	1.38	9	37	23.0	a	10.8	b
	13I58	4.7x10 ⁻⁰⁷	2.72	2.32	5	39	23.4	a	10.6	b

805 ^x For each representative isolate, the standardized mycelial growth rate was adjusted to the Analytis
806 Beta model: $Y = d \times (T - T_{min})^a \times (T_{max} - T)^b$, where *d*, *a*, and *b* are the regression coefficients.

807 ^y Optimum growth temperature estimated by the adjusted model.

808 ^z Maximum growth rate estimated by the adjusted model.

809 ^w Mean values followed by different letters within a column are significantly different according
810 to Fisher's protected least significant difference test at $P < 0.05$.

811

812 **Fig. 1.** Seasonal latent infections of *Colletotrichum* spp. on citrus twigs and leaves in Fresno, Kern,
813 and Tulare counties. Vertical bars represent the number of latent infections per leaf (LI/leaf)
814 recorded in mandarin and orange leaves in each season. Lines represent incidence (%) on mandarin
815 and orange twigs in each season. Vertical bars represent standard errors.

816 **Fig. 2.** A Bayesian inference phylogenetic tree of the *Colletotrichum boninense* species complex.
817 The phylogenetic tree was built using concatenated sequences of the ITS region and, the GAPDH
818 and TUB2 partial genes. Bayesian inference (BI) posterior values above 0.9 and bootstrap support
819 values from maximum likelihood (ML) above 80% are shown at each node (BI/ML). *C.*
820 *gloeosporioides* ICMP 17821 was used as the outgroup. (*) Indicates the ex-type strains. Isolates
821 from this study are shown in bold.

822 **Fig. 3.** A Bayesian inference phylogenetic tree of the *Colletotrichum gloeosporioides* species
823 complex. The phylogenetic tree was built using concatenated sequences of the ITS region and, the
824 GAPDH and TUB2 partial genes. Bayesian inference (BI) posterior values above 0.9 and bootstrap
825 support values from maximum likelihood (ML) above 80% are shown at each node (BI/ML). *C.*
826 *boninense* CBS 123755 was used as the outgroup. (*) Indicates the ex-type strains. Isolates from
827 this study are shown in bold.

828 **Fig.4.** Effect of temperature on the mycelial growth rate of *Colletotrichum gloeosporioides* and *C.*
829 *karstii*. For each species, data from the three representative isolates were combined and the
830 averaged growth rate was adjusted to a non-linear regression curve using the Analytis Beta Model.
831 For each isolate, data points indicate the mean of three independents sets with three replicates each,
832 and vertical bars showed their respective standard error.

833 **Fig. 5.** Effect of temperature on conidial germination (A) and appressoria formation (B) of *C.*
834 *gloeosporioides* and *C. karstii*. The shaded areas showed the 95% confidence interval around the
835 smooth line.

836 **Fig. 6.** Relative growth inhibition (%) of *Colletotrichum gloeosporioides* and *C. karstii* on culture
837 media amended with chlorothalonil, fluopyram, metconazole, penthiopyrad, Cu hydroxide, and
838 tebuconazole. For each fungicide, points represent the average of 21 *C. gloeosporioides* isolates
839 and 32 *C. karstii* (B) isolates, and the lines represent the standard deviation.

840 **Fig. 7.** Effective concentration ($\mu\text{g ml}^{-1}$) that results in 50% mycelial growth inhibition (EC_{50}) of
841 *Colletotrichum gloeosporioides* and *C. karstii* for chlorothalonil (A), fluopyram (B), metconazole
842 (C), penthiopyrad (D), Cu hydroxide (E), and tebuconazole. For each fungicide and pathogen,
843 points represent the average of 16 isolates, and the lines represent the 95% confidence intervals.

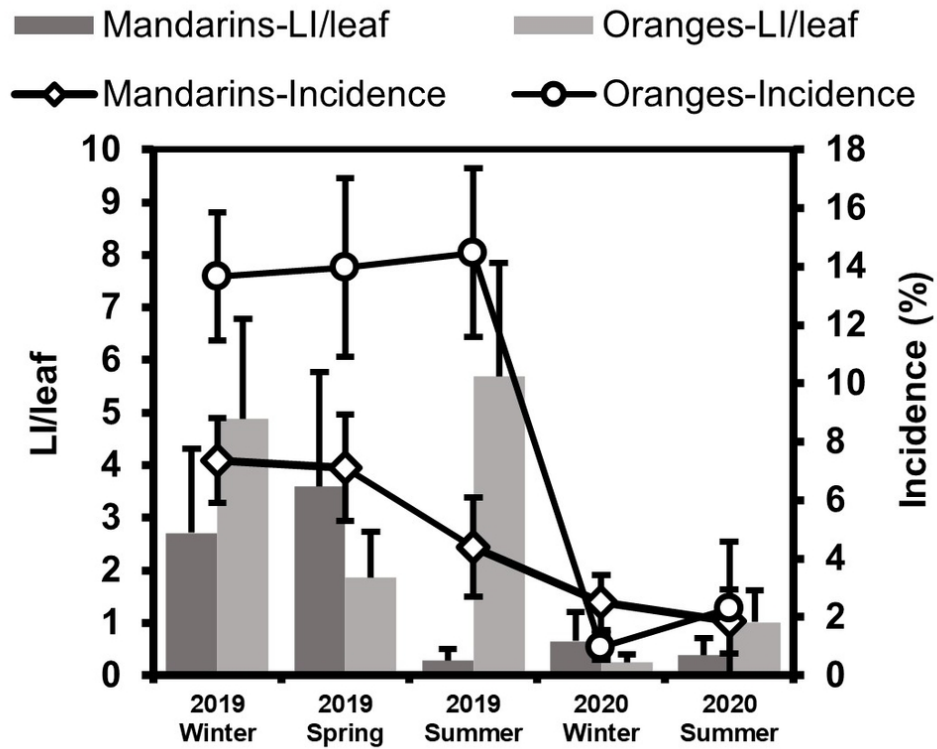


Fig. 1. Seasonal latent infections of *Colletotrichum* spp. on citrus twigs and leaves in Fresno, Kern, and Tulare counties. Vertical bars represent the number of latent infections per leaf (LI/leaf) recorded in mandarin and orange leaves in each season. Lines represent incidence (%) on mandarin and orange twigs in each season. Vertical bars represent standard errors.

85x69mm (300 x 300 DPI)

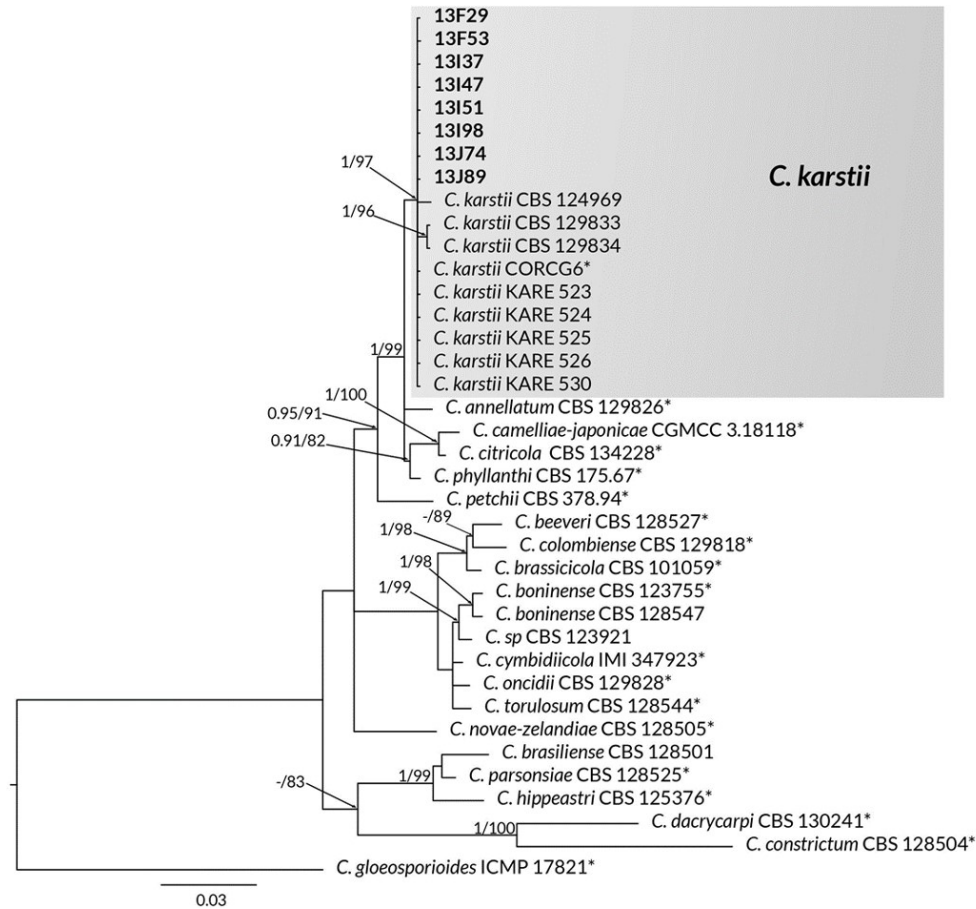


Fig. 2. A Bayesian inference phylogenetic tree of the *Colletotrichum boninense* species complex. The phylogenetic tree was built using concatenated sequences of the ITS region and, the GAPDH and TUB2 partial genes. Bayesian inference (BI) posterior values above 0.9 and bootstrap support values from maximum likelihood (ML) above 80% are shown at each node (BI/ML). *C. gloeosporioides* ICMP 17821 was used as the outgroup. (*) Indicates the ex-type strains. Isolates from this study are shown in bold.

177x160mm (150 x 150 DPI)



Fig. 3. A Bayesian inference phylogenetic tree of the *Colletotrichum gloeosporioides* species complex. The phylogenetic tree was built using concatenated sequences of the ITS region and, the GAPDH and TUB2 partial genes. Bayesian inference (BI) posterior values above 0.9 and bootstrap support values from maximum likelihood (ML) above 80% are shown at each node (BI/ML). *C. boninense* CBS 123755 was used as the outgroup. (*) Indicates the ex-type strains. Isolates from this study are shown in bold.

177x179mm (330 x 330 DPI)

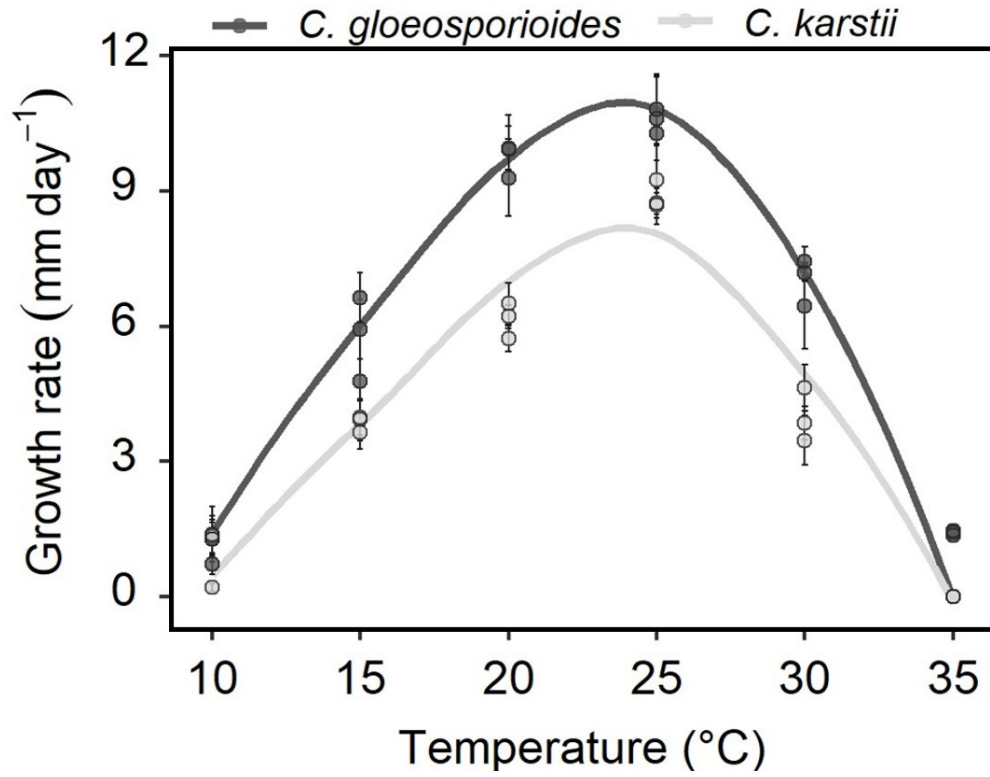


Fig.4. Effect of temperature on the mycelial growth rate of *Colletotrichum gloeosporioides* s.s. and *C. karstii*. For each species, data from the three representative isolates were combined and the averaged growth rate was adjusted to a non-linear regression curve using the Analytis Beta Model. For each isolate, data points indicate the mean of three independent sets with three replicates each, and vertical bars showed their respective standard error.

82x63mm (330 x 330 DPI)

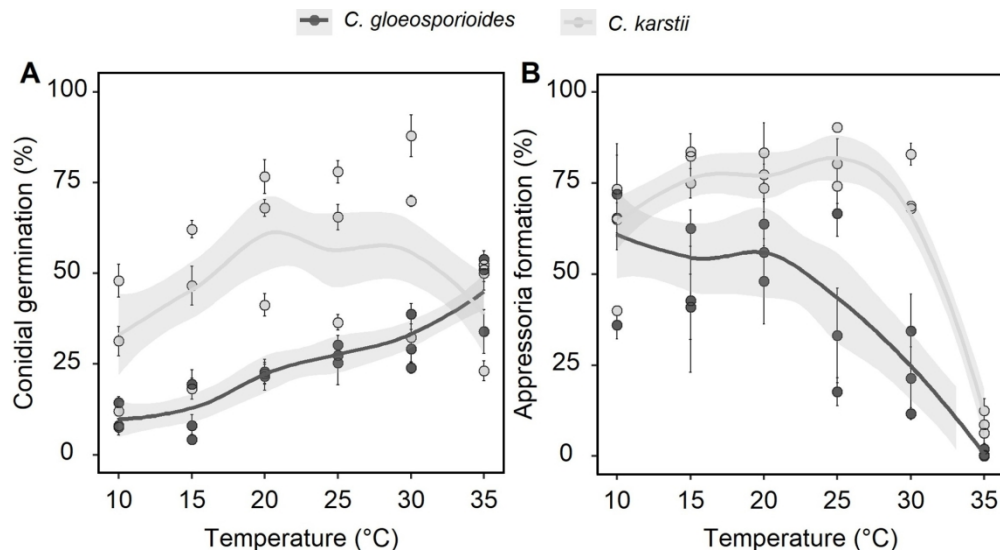


Fig. 5. Effect of temperature on conidial germination (A) and appressoria formation (B) of *C. gloeosporioides* s.s. and *C. karstii*. The shaded areas showed the 95% confidence interval around the smooth line.

177x96mm (330 x 330 DPI)

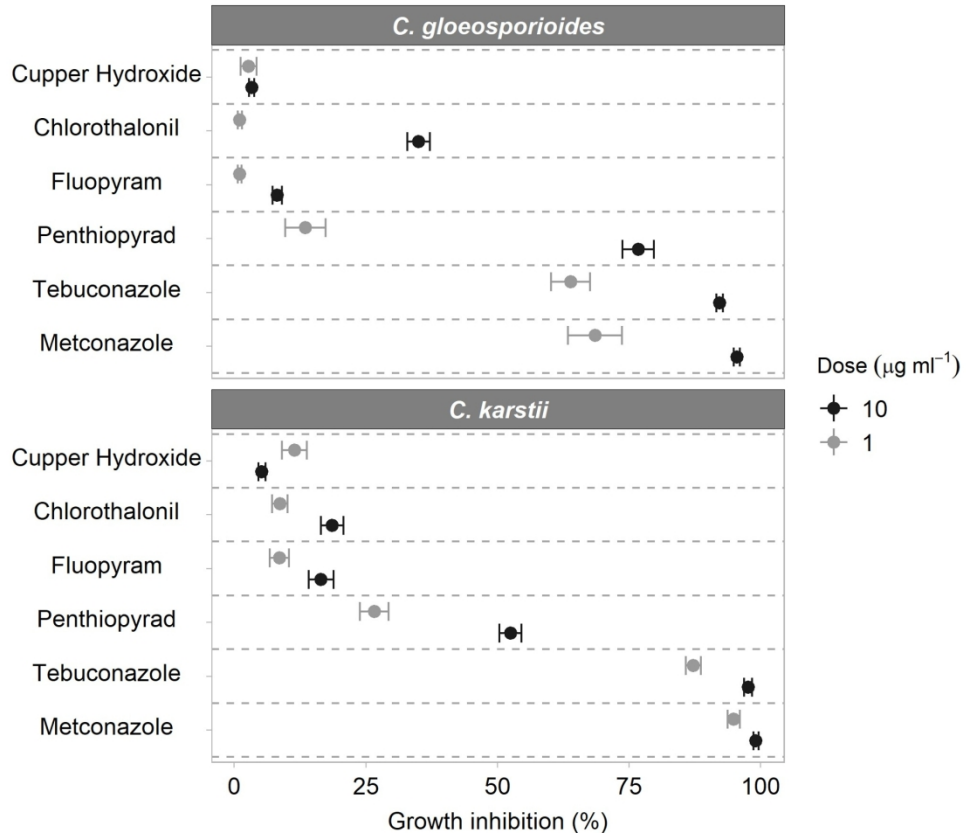


Fig. 6. Relative growth inhibition (%) of *Colletotrichum gloeosporioides* s.l. and *C. karstii* on culture media amended with chlorothalonil, fluopyram, metconazole, penthiopyrad, Cu hydroxide, and tebuconazole. For each fungicide, points represent the average of 21 *C. gloeosporioides* s.l. isolates and 32 *C. karstii* (B) isolates, and the lines represent the standard deviation.

177x148mm (300 x 300 DPI)

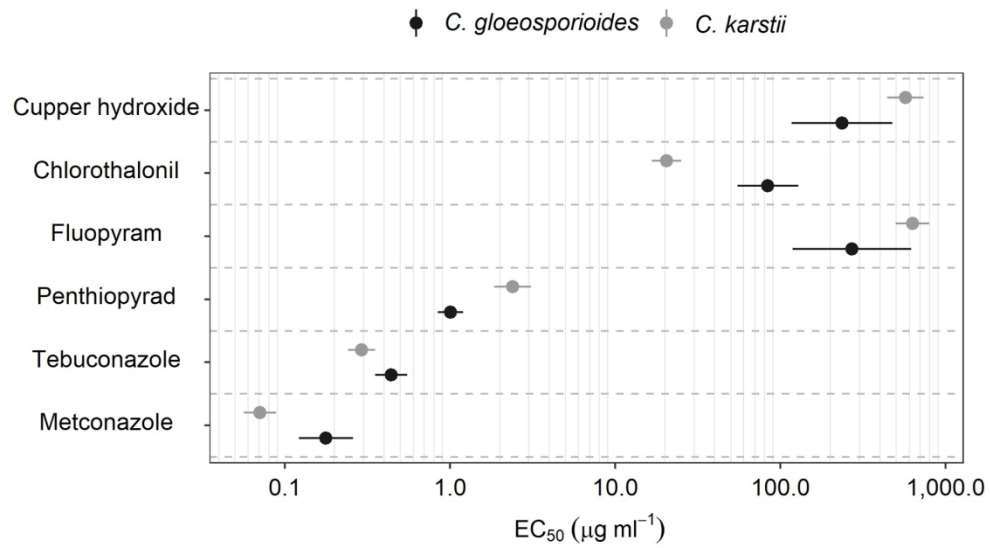


Fig. 7. Effective concentration ($\mu\text{g ml}^{-1}$) that results in 50% mycelial growth inhibition (EC_{50}) of *Colletotrichum gloeosporioides* s.l. and *C. karstii* for chlorothalonil (A), fluopyram (B), metconazole (C), penthiopyrad (D), Cu hydroxide (E), and tebuconazole. For each fungicide and pathogen, points represent the average of 16 isolates, and the lines represent the 95% confidence intervals.

177x98mm (300 x 300 DPI)

TABLE S1. Isolates of *Colletotrichum* spp. used in this study.

Isolate	Morphologic al group*	Species complex *	Species *	Location	Host	Cultivar	Tissue
13F28 ^{y,z}	1	<i>C. boninense</i>	<i>C. karstii</i>	Fresno	<i>C. sinensis</i>	Cara Cara	Twig
13F29 ^{v,w,x}	1	<i>C. boninense</i>	<i>C. karstii</i>	Fresno	<i>C. sinensis</i>	Cara Cara	Twig
13F30	1	<i>C. boninense</i>	<i>C. karstii</i>	Fresno	<i>C. sinensis</i>	Cara Cara	Twig
13F53 ^{v,w,y,z}	1	<i>C. boninense</i>	<i>C. karstii</i>	Fresno	<i>C. reticulata</i>	Owari Satsuma	Leaf
13F54 ^{v,y}	1	<i>C. boninense</i>	<i>C. karstii</i>	Fresno	<i>C. limon</i>	Lisbon	Leaf
13F57 ^{y,z}	1	<i>C. boninense</i>	<i>C. karstii</i>	Fresno	<i>C. reticulata</i>	Tango	Twig
13G09	1	<i>C. boninense</i>	<i>C. karstii</i>	Fresno	<i>C. reticulata</i>	Tango	Leaf
13G11	1	<i>C. boninense</i>	<i>C. karstii</i>	Fresno	<i>C. limon</i>	Lisbon	Leaf
13G12	1	<i>C. boninense</i>	<i>C. karstii</i>	Fresno	<i>C. limon</i>	Lisbon	Leaf
13G13	1	<i>C. boninense</i>	<i>C. karstii</i>	Fresno	<i>C. limon</i>	Lisbon	Leaf
13G15	1	<i>C. boninense</i>	<i>C. karstii</i>	Fresno	<i>C. limon</i>	Lisbon	Leaf
13G16 ^y	1	<i>C. boninense</i>	<i>C. karstii</i>	Fresno	<i>C. reticulata</i>	Owari Satsuma	Leaf
13G17 ^y	1	<i>C. boninense</i>	<i>C. karstii</i>	Fresno	<i>C. reticulata</i>	Gold Nugget	Leaf
13G18	1	<i>C. boninense</i>	<i>C. karstii</i>	Fresno	<i>C. reticulata</i>	Tango	Leaf
13G25 ^{v,y,z}	1	<i>C. boninense</i>	<i>C. karstii</i>	Fresno	<i>C. sinensis</i>	Cara Cara	leaf
13G35	1	<i>C. boninense</i>	<i>C. karstii</i>	Fresno	<i>C. limon</i>	Lisbon	Leaf
13G37 ^{y,z}	1	<i>C. boninense</i>	<i>C. karstii</i>	Fresno	<i>C. reticulata</i>	Tango	Leaf
13G40	1	<i>C. boninense</i>	<i>C. karstii</i>	Fresno	<i>C. sinensis</i>	Cara Cara	Leaf
13H73 ^{y,z}	1	<i>C. boninense</i>	<i>C. karstii</i>	Kern	<i>C. reticulata</i>	Owari Satsuma	Leaf
13I36	1	<i>C. boninense</i>	<i>C. karstii</i>	Tulare	<i>C. reticulata</i>	Sumo	Leaf
13I37 ^w	1	<i>C. boninense</i>	<i>C. karstii</i>	Tulare	<i>C. reticulata</i>	Sumo	Leaf
13I47 ^{v,w}	1	<i>C. boninense</i>	<i>C. karstii</i>	Tulare	<i>C. reticulata</i>	Tango	Leaf
13I48	1	<i>C. boninense</i>	<i>C. karstii</i>	Tulare	<i>C. sinensis</i>	Washington	Leaf
13I51 ^w	1	<i>C. boninense</i>	<i>C. karstii</i>	Tulare	<i>C. reticulata</i>	Sumo	Leaf
13I98 ^w	1	<i>C. boninense</i>	<i>C. karstii</i>	Tulare	<i>C. sinensis</i>	Washington	Twig
13I99	1	<i>C. boninense</i>	<i>C. karstii</i>	Tulare	<i>C. sinensis</i>	Cara Cara	Twig
13I100 ^v	1	<i>C. boninense</i>	<i>C. karstii</i>	Tulare	<i>C. reticulata</i>	Tango	Twig
13J02 ^{v,y}	1	<i>C. boninense</i>	<i>C. karstii</i>	Tulare	<i>C. sinensis</i>	Cara Cara	Twig
13J03	1	<i>C. boninense</i>	<i>C. karstii</i>	Tulare	<i>C. reticulata</i>	Tango	Twig
13J04	1	<i>C. boninense</i>	<i>C. karstii</i>	Tulare	<i>C. reticulata</i>	Tango	Twig

13J06	1	<i>C. boninense</i>	<i>C. karstii</i>	Tulare	<i>C. sinensis</i>	Cara Cara	Twig
13J07 ^{y,z}	1	<i>C. boninense</i>	<i>C. karstii</i>	Tulare	<i>C. reticulata</i>	Clemenules	Twig
13J08	1	<i>C. boninense</i>	<i>C. karstii</i>	Tulare	<i>C. sinensis</i>	Atwood	Twig
13J09	1	<i>C. boninense</i>	<i>C. karstii</i>	Tulare	<i>C. sinensis</i>	Atwood	Twig
13J10	1	<i>C. boninense</i>	<i>C. karstii</i>	Tulare	<i>C. reticulata</i>	Gold Nugget	Twig
13J12 ^{v,y,z}	1	<i>C. boninense</i>	<i>C. karstii</i>	Tulare	<i>C. sinensis</i>	Fukumoto	Twig
13J13	1	<i>C. boninense</i>	<i>C. karstii</i>	Tulare	<i>C. sinensis</i>	Cara Cara	Twig
13J14	1	<i>C. boninense</i>	<i>C. karstii</i>	Tulare	<i>C. sinensis</i>	Washington	Twig
13J15 ^{v,y}	1	<i>C. boninense</i>	<i>C. karstii</i>	Tulare	<i>C. sinensis</i>	Fukumoto	Twig
13J39	1	<i>C. boninense</i>	<i>C. karstii</i>	Tulare	<i>C. reticulata</i>	Tango	Twig
13J42 ^v	1	<i>C. boninense</i>	<i>C. karstii</i>	Tulare	<i>C. reticulata</i>	Tango	Leaf
13J43 ^{v,y}	1	<i>C. boninense</i>	<i>C. karstii</i>	Tulare	<i>C. sinensis</i>	Cara Cara	Leaf
13J44 ^v	1	<i>C. boninense</i>	<i>C. karstii</i>	Tulare	<i>C. reticulata</i>	Tango	Leaf
13J48	1	<i>C. boninense</i>	<i>C. karstii</i>	Kern	<i>C. sinensis</i>	Atwood	Twig
13J51	1	<i>C. boninense</i>	<i>C. karstii</i>	Tulare	<i>C. sinensis</i>	Washington	Twig
13J60	1	<i>C. boninense</i>	<i>C. karstii</i>	Tulare	<i>C. sinensis</i>	Washington	Twig
13J68	1	<i>C. boninense</i>	<i>C. karstii</i>	Kern	<i>C. sinensis</i>	Atwood	Twig
13J73 ^v	1	<i>C. boninense</i>	<i>C. karstii</i>	Kern	<i>C. sinensis</i>	Atwood	Twig
13J74 ^{v,w,x}	1	<i>C. boninense</i>	<i>C. karstii</i>	Fresno	<i>C. reticulata</i>	Clemenules	Twig
13J78	1	<i>C. boninense</i>	<i>C. karstii</i>	Tulare	<i>C. sinensis</i>	Washington	Twig
13J83	1	<i>C. boninense</i>	<i>C. karstii</i>	Twig
13J84	1	<i>C. boninense</i>	<i>C. karstii</i>	Twig
13J87	1	<i>C. boninense</i>	<i>C. karstii</i>	Tulare	<i>C. sinensis</i>	Washington	Twig
13J89 ^{v,w,x}	1	<i>C. boninense</i>	<i>C. karstii</i>	Fresno	<i>C. reticulata</i>	Clemenules	Leaf
13K59	1	<i>C. boninense</i>	<i>C. karstii</i>	Fresno	<i>C. reticulata</i>	Tango	Twig
13K65	1	<i>C. boninense</i>	<i>C. karstii</i>	Kern	<i>C. sinensis</i>	Atwood	Twig
13K66	1	<i>C. boninense</i>	<i>C. karstii</i>	Kern	<i>C. sinensis</i>	Atwood	Twig
13L06	1	<i>C. boninense</i>	<i>C. karstii</i>	Kern	<i>C. sinensis</i>	Atwood	Twig
13L07	1	<i>C. boninense</i>	<i>C. karstii</i>	Kern	<i>C. sinensis</i>	Atwood	Twig
13L08	1	<i>C. boninense</i>	<i>C. karstii</i>	Tulare	<i>C. sinensis</i>	Cara Cara	Twig
13L09	1	<i>C. boninense</i>	<i>C. karstii</i>	Tulare	<i>C. sinensis</i>	Cara Cara	Twig
13L10	1	<i>C. boninense</i>	<i>C. karstii</i>	Tulare	<i>C. sinensis</i>	Washington	Twig
14E03 ^y	1	<i>C. boninense</i>	<i>C. karstii</i>	Tulare	<i>C. reticulata</i>	Tango	Leaf
14E04 ^y	1	<i>C. boninense</i>	<i>C. karstii</i>	Tulare	<i>C. reticulata</i>	Tango	Twigs
14E05 ^y	1	<i>C. boninense</i>	<i>C. karstii</i>	Tulare	<i>C. reticulata</i>	Gold Nugget	Twigs

14E06 ^{y,z}	1	<i>C. boninense</i>	<i>C. karstii</i>	Tulare	<i>C. reticulata</i>	Gold Nugget	Twigs
14E07 ^y	1	<i>C. boninense</i>	<i>C. karstii</i>	Tulare	<i>C. reticulata</i>	Tango	Twigs
14E10 ^y	1	<i>C. boninense</i>	<i>C. karstii</i>	Tulare	<i>C. reticulata</i>	Gold Nugget	Twigs
14E11 ^y	1	<i>C. boninense</i>	<i>C. karstii</i>	Tulare	<i>C. reticulata</i>	Gold Nugget	Twigs
14E12 ^{y,z}	1	<i>C. boninense</i>	<i>C. karstii</i>	Tulare	<i>C. reticulata</i>	Gold Nugget	Twigs
14E13 ^{y,z}	1	<i>C. boninense</i>	<i>C. karstii</i>	Tulare	<i>C. reticulata</i>	Tango	Leaf
14E14 ^y	1	<i>C. boninense</i>	<i>C. karstii</i>	Tulare	<i>C. reticulata</i>	Gold Nugget	Leaf
14E15 ^y	1	<i>C. boninense</i>	<i>C. karstii</i>	Tulare	<i>C. reticulata</i>	Gold Nugget	Twigs
14E16 ^{y,z}	1	<i>C. boninense</i>	<i>C. karstii</i>	Tulare	<i>C. reticulata</i>	Gold Nugget	Twigs
14E18 ^y	1	<i>C. boninense</i>	<i>C. karstii</i>	Tulare	<i>C. reticulata</i>	Tango	Leaf
14E19 ^{y,z}	1	<i>C. boninense</i>	<i>C. karstii</i>	Tulare	<i>C. reticulata</i>	Tango	Leaf
14E21 ^{y,z}	1	<i>C. boninense</i>	<i>C. karstii</i>	Tulare	<i>C. reticulata</i>	Gold Nugget	Twigs
14E25 ^{y,z}	1	<i>C. boninense</i>	<i>C. karstii</i>	Tulare	<i>C. reticulata</i>	Tango	Twigs
14E27 ^{y,z}	1	<i>C. boninense</i>	<i>C. karstii</i>	Tulare	<i>C. reticulata</i>	Gold Nugget	Leaf
14E28 ^y	1	<i>C. boninense</i>	<i>C. karstii</i>	Tulare	<i>C. reticulata</i>	Gold Nugget	Leaf
13F33 ^{y,z}	2	<i>C. gloeosporioides</i>	<i>C. gloeosporioides</i>	Fresno	<i>C. sinensis</i>	Cara Cara	Twig
13F41 ^{y,z}	2	<i>C. gloeosporioides</i>	<i>C. gloeosporioides</i>	Fresno	<i>C. sinensis</i>	Cara Cara	Leaf
13G24 ^{v,y,z}	2	<i>C. gloeosporioides</i>	<i>C. gloeosporioides</i>	Twig
13G36 ^{v,w,y,z}	2	<i>C. gloeosporioides</i>	<i>C. gloeosporioides</i>	Fresno	<i>C. reticulata</i>	Tango	Leaf
13G88 ^{y,z}	2	<i>C. gloeosporioides</i>	<i>C. gloeosporioides</i>	Tulare	<i>C. reticulata</i>	Gold Nugget	Twig
13I33 ^{y,z}	2	<i>C. gloeosporioides</i>	<i>C. gloeosporioides</i>	Tulare	<i>C. sinensis</i>	Fukumoto	Leaf
13I35 ^{y,z}	2	<i>C. gloeosporioides</i>	<i>C. gloeosporioides</i>	Tulare	<i>C. sinensis</i>	Cara Cara	Leaf
13I45 ^{v,w,y}	2	<i>C. gloeosporioides</i>	<i>C. gloeosporioides</i>	Tulare	<i>C. sinensis</i>	Atwood	Leaf
13I46 ^{v,w,x,y,z}	2	<i>C. gloeosporioides</i>	<i>C. gloeosporioides</i>	Tulare	<i>C. sinensis</i>	Atwood	Leaf
13I49 ^{w,y,z}	2	<i>C. gloeosporioides</i>	<i>C. gloeosporioides</i>	Tulare	<i>C. reticulata</i>	Clemenules	Leaf
13I50 ^{v,w,y}	2	<i>C. gloeosporioides</i>	<i>C. gloeosporioides</i>	Tulare	<i>C. reticulata</i>	Clemenules	Leaf
13I56 ^{v,w,y,z}	2	<i>C. gloeosporioides</i>	<i>C. gloeosporioides</i>	Tulare	<i>C. reticulata</i>	Tango	Twig
13I57 ^{v,w,y,z}	2	<i>C. gloeosporioides</i>	<i>C. gloeosporioides</i>	Tulare	<i>C. sinensis</i>	Washington	Leaf
13I58 ^{v,w,x,y,z}	2	<i>C. gloeosporioides</i>	<i>C. gloeosporioides</i>	Tulare	<i>C. sinensis</i>	Fukumoto	Leaf
13J05 ^{v,y}	2	<i>C. gloeosporioides</i>	<i>C. gloeosporioides</i>	Tulare	<i>C. sinensis</i>	Cara Cara	Twig
13J11 ^{v,y}	2	<i>C. gloeosporioides</i>	<i>C. gloeosporioides</i>	Tulare	<i>C. reticulata</i>	Clemenules	Twig
13J41 ^{v,y,z}	2	<i>C. gloeosporioides</i>	<i>C. gloeosporioides</i>	Tulare	<i>C. reticulata</i>	Clemenules	Twig
13J50 ^y	2	<i>C. gloeosporioides</i>	<i>C. gloeosporioides</i>	Tulare	<i>C. reticulata</i>	Clemenules	Twig
13J55 ^{v,w,y,z}	2	<i>C. gloeosporioides</i>	<i>C. gloeosporioides</i>	Tulare	<i>C. sinensis</i>	Washington	Twig

13J65 ^{v, w, y, z}	2	<i>C. gloeosporioides</i>	<i>C. gloeosporioides</i>	Tulare	<i>C. reticulata</i>	Tango	Twig
13J85 ^{v, w, x, y, z}	2	<i>C. gloeosporioides</i>	<i>C. gloeosporioides</i>	Tulare	<i>C. reticulata</i>	Tango	Twig
13J88 ^{v, y}	2	<i>C. gloeosporioides</i>	<i>C. gloeosporioides</i>	Twig

^v Isolates used for morphological characterization and pathogenicity tests.

^w Isolates used for molecular characterization.

^x Isolates selected as representative isolates.

^y Isolates used in experiments performed to evaluate the effect of fungicides on spore germination and mycelium growth (agar dilution method).

^z Isolates used to determine the 50% effective fungicide concentration (EC₅₀) for each fungicide.

* Classification based on morphological characteristics.